Nuclear Instruments and Methods in Physics Research A 372 (1996) 349–351

NUCLEAR INSTRUMENTS & METHODS IN PHYSICS RESEARCH Section A

A movable polarized target for high energy spin physics experiments

N.A. Bazhanov[a], B. Benda[b], N.S. Borisov[c], A.P. Dzyubak[d], G. Durand[b], L.B. Golovanov[e], G.M. Gurevich[f], A.I. Kovalev[a], A.B. Lazarev[c], F. Lehar[b], A.A. Lukhanin[d], A.B. Neganov[c], S.V. Topalov[f], S.N. Shilov[c], Yu.A. Usov[c,*]

[a]*Physics Dept., Petersburg Nuclear Physics Inst., 188350 Gatchina, Russia*
[b]*CEA DSM-DAPNIA, CE Saclay, 91191 Gif-sur-Yvette Cedex, France*
[c]*Laboratory of Nuclear Problems, JINR, 141980 Dubna, Moscow Region, Russia*
[d]*Kharkov Institute of Physics and Technology, Academicheskaya str. 1, 310108 Kharkov, Ukraine*
[e]*Laboratory of High Energy Physics, JINR, 141980 Dubna, Moscow Region, Russia*
[f]*Institute for Nuclear Research, Russian Academy of Sciences, 60th October anniversary prosp. 7A, 117312 Moscow, Russia*

Received 26 October 1995

Abstract

A movable polarized target has a volume 140 cm^3 (20 cm long and 3 cm diameter). Polarizing magnet was tested to 6.5 T, homogeneity is better than 2×10^{-4}. The nuclear spin relaxation time in a frozen mode (at a temperature 50 mK and magnetic field 2.5 T) is over 1000 h. Maximum values of proton polarization obtained were 80% and 85% for positive and negative polarization, respectively.

The accelerator complex of the Joint Institute for Nuclear Research (JINR) in Dubna becomes now a unique place to provide 3–12 GeV/c polarized deuteron beams with high intensity and good polarization. It is possible to obtain quasi-monoenergetic neutron and proton beams too using a break-up of accelerated deuterons. A new generation of experiments can be carried out at this accelerator complex [1].

To get full benefit of this opportunity, the experiments with polarized beams must be performed in conjunction with polarized proton or deuteron targets. To produce in a shortest possible time a working combination of a polarized beam and polarized target, it was agreed to use, after reconstruction, the Saclay–Argonne frozen spin proton polarized target which was built for and used initially in an experiment at FERMILAB (USA) [2].

For the purposes of the physics program in Dubna the target has been reassembled and upgraded adding the missing parts. A new quality was given to the target assembly during this reconstruction – a transportability from one experimental area to another. This is a "movable" polarized target (MPT) concept. It means that all the major parts of the target assembly disposed closely to the beam line (target cell inside a $^3He/^4He$ dilution refrigerator, magnets, power supplies, service liquid helium dewars, ^3He pumps etc.) are mounted on two separate decks (Fig. 1) which can be moved as blocks in and out of the beam, and also between various accelerators. These decks may be translated on high precision rails fixed on a main frame. During the experiment, the working target may be moved in or out of the beamline within some minutes without interference with the polarizing or frozen spin mode in process. Between experiments, transportation to another area does not need disassembly of the equipped decks. The dimensions of the decks with their equipments correspond to dimensions of a standard sea container.

Larger of two decks contains the $^3He/^4He$ dilution refrigerator with a horizontal axis mounted on a 1.5 tons concrete cube, a 30 l service helium dewar of the refrigerator, a 1000 l supply helium dewar and a ^3He pumping system. The pumping system consisting of one Geraer compressorenwerk (RPW3600) 3600 l/s roots pump and two Leybold pumps (WS-1000 and WS-250) with pumping speeds 1000 l/s and 250 l/s mounted on a compact stage and placed onto the deck using pneumatic dampers for vibration isolation, similar to that in Ref. [3]. The pumping system is connected to the dilution refrigerator through about 1.5 m piece of 200 mm diameter stainless steel tube with bellows inserts. A quality of the

* Corresponding author. Tel. +7 09621 63233, e-mail usov@main1.jinr.dubna.su.

SSDI 0168-9002(95)01307-5

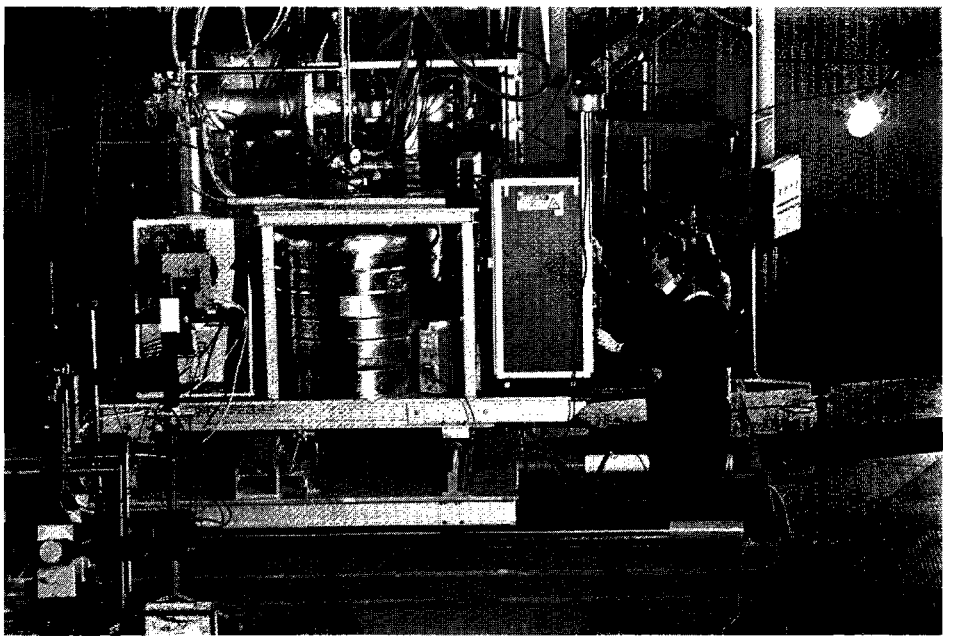

Fig. 1. Photograph of the movable polarized target.

vibration isolation is demonstrated by the fact that it was possible to work in a frozen polarization mode at a working temperature $\leq$50 mK without any additional thermal load to the refrigerator, and small phonic noise on the NMR coils.

A polarizing superconducting solenoid, its 300 l service helium dewar and power supply are mounted on a smaller deck. For easier operation and for good access to the physics detectors, the equipment, that is not mounted on the decks, is placed outside of the radiation controlled area.

A remote control of the entire operation of the MPT was achieved from the control room installed inside the trailer. It contains an operating vacuum, ^{3}He and ^{4}He systems, an interlock system, a microwave system, and a NMR system. A new powerful two-arm cleaning system for ^{3}He was built containing liquid nitrogen cooled charcoal traps and warm silicagel traps.

The microwave system intended for proton polarization buildup consists of a microwave source, a waveguide, and a power supply. A diffraction radiation generator with 4 mm wavelength was used as the microwave source. Its main characteristics are:

- frequency range: 70–78 GHz,
- output power: no less than 5 W,
- relative frequency instability: no more than 10^{-5},
- FWHM of a radiation line: no more than 0.5 MHz.

The waveguide consists of warm and cold parts. The warm part contains a directed brancher intended to measure the frequency, an electronic attenuator, and a wavemode transformer. The microwave power comes to the refrigerator in H01 mode. The cold part of the waveguide inside the refrigerator was left unchanged. 1,2-propanediol with a paramagnetic Cr(5) impurity having a spin concentration of 1.5×10^{20} cm^{-3} was used as a target material [4]. A load of 140 cm^3 of propanediol beads in a plastic container having 200 mm length and 30 mm diameter was placed inside the dilution refrigerator.

The target polarization measurements were carried out using a computer controlled NMR system. Maximum values of proton polarization obtained were 80 and 85% for positive and negative polarizations, respectively. Difference of microwave frequencies corresponding to polarization maxima was measured to be 340 MHz. A duration of one continuous run at a given sign of target polarization was about 12 h. Polarization degradation during this period was insignificant since the nuclear spin relaxation time in a frozen mode (at a temperature 50 mK and magnetic field 2.5 T) is over 1000 h.

First experiment using MPT and polarized neutron beam of JINR accelerator complex has been done in February 1995. The difference in the transmission cross sections of polarized neutrons through the polarized proton target when beam and target polarization directions are parallel or antiparallel has been measured. All the work on target reconstruction, its transfer to the beam line and the first experiment have taken approximately 8 months.

For further experiments transverse polarization of protons (and deuterons) is needed. A set of holding coils for achieving transverse polarization, as well as a new polarizing solenoid, are being built.

Acknowledgements

The authors express their gratitude to Profs. A.M. Baldin, J. Haissinsky, I.M. Karnaukhov, Ph. Leconte, N.M. Piskunov, V.S. Rumyantsev, N.A. Russakovich, A.N. Sissakyan, P.V. Sorokin for their help and support with the work. The authors are also grateful to Yu. Borzunov, E.I. Bunyatova, V.F. Burinov, V. Korniyenkov, V.N. Matafonov, Yu.A. Plis, V.V. Polyakov, V.V. Teterin, V.Yu. Trautman and A. Tsvinev for their assistance in carrying out the experiments.

Work is supported by INTAS under grant 93-3315.

References

[1] F. Lehar et al., Nucl. Instr. and Meth. A 356 (1995) 58.
[2] P. Chaumette et al., Proc. 8th Int. Symp. on High Energy Spin Physics, Minneapolis, Minnesota (1988).
[3] N.S. Borisov, V.V. Kulikov, A.B. Neganov and Yu.A. Usov, Cryogenics 33 (1993) 738.
[4] E.I. Bunytova et al., Preprint JINR 12–82–732, Dubna (1982).

Z. Phys. C 71, 65–74 (1996)

ZEITSCHRIFT
FÜR PHYSIK C

Measurement of the total cross section difference $\Delta\sigma_L$ in *np* transmission at 1.19, 2.49 and 3.65 GeV

B.P. Adiasevich[4], V.G. Antonenko[4], S.A. Averichev[1], L.S. Azhgirey[2], J. Ball[5], N.A. Bazhanov[6], B. Benda[3], N.S. Borisov[2], Yu.T. Borzunov[1], E.I. Bunyatova[2], V.F. Burinov[2], E.V. Chernykh[1], S.A. Dolgii[1], G. Durand[3], A.P. Dzyubak[7], A.N. Fedorov[8], V.V. Fimushkin[1], J.M. Fontaine[5], V.V. Glagolev[1], L.B. Golovanov[1], D.P. Grosnick[9], G.M. Gurevich[10], D.A. Hill[9], A.V. Karpunin[1], T.E. Kasprzyk[9], B.A. Khachaturov[2], A.D. Kirillov[1], N.I. Kochelev[11], A.D. Kovalenko[1], A.I. Kovalev[6], M.V. Kulikov[1], V.P. Ladygin[1], A.B. Lazarev[2], F. Lehar[3], A. de Lesquen[3], M.Yu. Liburg[1], D. Lopiano[9], A.A. Lukhanin[7], P.K. Maniakov[1], V.N. Matafonov[2], E.A. Matyushevsky[1], G. Mgebrishvili[4], S.V. Mironov[1], A.B. Neganov[2], G.P. Nikolaevsky[1], A.A. Nomofilov[1], Yu.K. Pilipenko[1], I.L. Pisarev[2], N.M. Piskunov[1], Yu.A. Plis[2], Yu.P. Polunin[4], V.V. Polyakov[6], A.N. Prokofiev[6], D.A. Ronzhin[2], P.A. Rukoyatkin[1], J.L. Sans[5], V.I. Sharov[1], S.N. Shilov[2], Yu.A. Shishov[1], V.B. Shutov[1], P.V. Sorokin[7], H.M. Spinka[9], A.Yu. Starikov[1], G.D. Stoletov[2], E.A. Strokovsky[1], L.N. Strunov[1], A.L. Svetov[1], V.V. Teterin[2], S.V. Topalov[10], V.Yu. Trautman[6], A.P. Tsvinev[1], Yu.A. Usov[2], V.V. Vikhrov[6], V.I. Volkov[1], A.A. Yershov[12], V.P. Yershov[1], S.A. Zaporozhets[1], A.A. Zhdanov[6]

[1]Laboratory of High Energies, JINR, 141980 Dubna, Moscow Region, Russia
[2]Laboratory of Nuclear Problems, JINR, 141980 Dubna, Moscow Region, Russia
[3]CEA-DAPNIA, CE Saclay, F-91191 Gif sur Yvette Cedex, France
[4]I.V.Kurchatov Institute of Atomic Energy, Kurchatova str. 46, 123182 Moscow, Russia
[5]Laboratoire National SATURNE, CNRS/IN2P3 and CEA/DSM, CE Saclay, F-91191 Gif sur Yvette Cedex, France
[6]Petersburg Nuclear Physics Institute, 188350, Gatchina, Russia
[7]Kharkov Institute of Physics and Technology, Academicheskaya str. 1, 310108 Kharkov, Ukraine
[8]Laboratory of Particle Physics, JINR, 141980 Dubna, Moscow Region, Russia
[9]ANL-HEP, 9700 South Cass Avenue, Argonne, IL 60439, USA
[10]Institute for Nuclear Research, Russian Academy of Sciences, 60th October Anniversary Prospect 7A, 117312 Moscow, Russia
[11]Laboratory of Theoretical Physics, JINR, 141980 Dubna, Moscow Region, Russia
[12]Institute of Nuclear Physics, Moscow State University, 119899 Moscow, Russia

Received: 28 February 1996

Abstract. Results of the total cross section difference $\Delta\sigma_L$ in a *np* transmission experiment at 1.19, 2.49 and 3.65 GeV incident neutron beam kinetic energies are presented. Measurements were performed at the Synchrophasotron of the Laboratory of High Energies of the Joint Institute for Nuclear Research in Dubna. Results were obtained with a polarized beam of free quasi-monochromatic neutrons passing through the new Dubna frozen spin proton target. The beam and target polarizations were oriented longitudinally. The present results were obtained at the highest energies of free polarized neutrons that can be reached at present. They extend the energy range of existing results from PSI, LAMPF and Saclay measured between 0.066 and 1.10 GeV. The new results are compared with $\Delta\sigma_L(pn)$ data determined as a difference between $\Delta\sigma_L(pd)$ and $\Delta\sigma_L(pp)$ ANL-ZGS measurements. The values of $\Delta\sigma_L$ for the isospin state $I = 0$ were deduced using known *pp* data.

1 Introduction

The aim of this paper is to present new results of the neutron-proton total cross section difference $\Delta\sigma_L$ measured with a quasi-monochromatic polarized neutron beam and a polarized proton target. Results were obtained at the central values of 1.19, 2.49 and 3.65 GeV neutron beam kinetic energies. The free polarized neutron beam was produced by break-up of polarized deuterons accelerated by the Synchrophasotron of the Laboratory of High Energies (LHE) of the Joint Institute for Nuclear Research (JINR) in Dubna. This accelerator provides the highest energy polarized neutron beam, which can be reached now [1]. The present experiment is the first one of series where the new Dubna polarized proton target was used.

The nucleon-nucleon (*NN*) total cross section differences $\Delta\sigma_T$ and $\Delta\sigma_L$ together with the spin-independent total cross section $\sigma_{0\text{tot}}$ are integral quantities linearly related with three non-vanishing imaginary parts of the *NN* forward scattering amplitudes via optical theorems. They are used for absolute normalization in any theoretical or phenomenological analysis. The observable $\sigma_{0\text{tot}}$ in *pp* and *np* interactions has been measured during the last fifty years over a very large energy region. The measurements of spin-dependent total cross section are rare due to a lack of polarized beams and targets. All three observables are measured in pure inclusive transmission experiments and need very high stability of detectors.

The total cross section differences for *pp* scattering were first measured at the ANL-ZGS and then in a few other laboratories: TRIUMF, PSI, LAMPF and

SATURNE II. Results cover the energy range from 0.2 to 12 GeV. Another point was measured at 200 GeV at FERMILAB for proton-proton and antiproton-proton interactions. Measurements with incident charged particles need a different experimental set-up than neutron-proton experiments due to the contribution of electromagnetic interactions. Existing results are discussed in [2] and in references therein. The isospin $I = 1$ data are also needed in order to deduce the isospin $I = 0$ quantities from *np* measurements.

Neutron-proton observables, $\Delta\sigma_T$ and $\Delta\sigma_L$ using free polarized neutrons, were first obtained in 1987 at SATURNE II yielding four points with relatively large errors [3]. These results have been completed by new accurate measurements at 9 to 10 energies, between 0.31 and 1.1 GeV for each observable [4, 5]. The Saclay results were soon followed by PSI measurements [6] in the energy region from 0.14 to 0.59 GeV with a continuous neutron energy spectrum [7]. The $\Delta\sigma_T(np)$ or $\Delta\sigma_L(np)$ data were collected simultaneously over the entire energy range. The PSI and Saclay sets allowed to deduce imaginary parts of *np* and $I = 0$ spin-dependent forward scattering amplitudes from 0.14 to 1.1 GeV [2, 5].

The observable $\Delta\sigma_L(np)$ has also been measured at five energies at LAMPF [8]. The measurements were done with a quasi-monoenergetic polarized neutron beam produced in $pd \Rightarrow n + X$ scattering of longitudinally polarized protons. Large neutron counter hodoscopes have to be used because of the small neutron beam intensity.

In addition, at low energies, the observable $\Delta\sigma_L(np)$ at 66 MeV was measured at the PSI preaccelerator [9], $\Delta\sigma_T(np)$ was determined at 9 energies between 3.8 and 11.6 MeV in TUNL [10,11] and at 16.2 MeV in Prague [12].

In fact, for the first time $\Delta\sigma_L(pn)$ results were deduced in 1981 from the $\Delta\sigma_L(pd)$ and $\Delta\sigma_L(pp)$ measurement at the ANL-ZGS [13]. Taking a simple difference between *pd* and *pp* results, corrected only for beam and target polarizations and for Coulomb-nuclear rescattering including deuteron break-up, yields data in fairly good agreement with free *np* data (see Sect. 6). Let us note that any correction for Glauber-type rescattering including 3-body state final interactions [14] provides a disagreement [2].

In Sect. 2 we shortly describe the phenomenology of the experiment. Section 3 treats the LHE polarized deuteron and neutron beams and beam polarization measurements. In Sect. 4 the new Dubna polarized proton target is described. The experimental set-up for the $\Delta\sigma_L(np)$ measurements with associated electronics are described in Sect. 5. The data analysis and systematic errors are treated in Sect. 6. Results and discussions are presented in Sect. 7.

2 Total cross section differences

Throughout this paper we use the nucleon-nucleon formalism and the four-spin notation of observables developed in [15].

The general expression of the total cross section for a polarized nucleon beam transmitted through a polarized proton target (PPT), with arbitrary directions of beam and target polarizations, was first deduced in [16, 17]. Taking into account fundamental conservation laws, it is written in [15] in the form:

$$\sigma_{\text{tot}} = \sigma_{0\text{tot}} + \sigma_{1\text{tot}}(\mathbf{P}_B, \mathbf{P}_T) + \sigma_{2\text{tot}}(\mathbf{P}_B, \mathbf{k})\,(\mathbf{P}_T, \mathbf{k}), \tag{2.1}$$

where $\mathbf{P}_B$ and $\mathbf{P}_T$ are the beam and target polarization vectors (more exactly pseudovectors), and $\mathbf{k}$ is the unit vector in the incident beam direction. The term $\sigma_{0\text{tot}}$ is the spin-independent total cross section, $\sigma_{1\text{tot}}$ and $\sigma_{2\text{tot}}$ are the spin dependent contributions. They are related to the forward scattering invariant amplitudes via optical theorems [15] :

$$\sigma_{0\text{tot}} = (2\pi/K)\,\text{Im}[a(0) + b(0)], \tag{2.2}$$

$$\sigma_{1\text{tot}} = (2\pi/K)\ \text{Im}[c(0) + d(0)], \tag{2.3}$$

$$\sigma_{2\text{tot}} = -(4\pi/K)\,\text{Im}[d(0)], \tag{2.4}$$

where K is the wave number in the CM system.

The total cross sections σ_{tot} and $\sigma_{0\text{tot}}$ are positive definite quantities. The spin-dependent contributions $\sigma_{1\text{tot}}$ and $\sigma_{2\text{tot}}$ are related to measurable quantities $\Delta\sigma_T$ and $\Delta\sigma_L$ by:

$$-\Delta\sigma_T = 2\sigma_{1\text{tot}}, \tag{2.5}$$

$$-\Delta\sigma_L = 2(\sigma_{1\text{tot}} + \sigma_{2\text{tot}}). \tag{2.6}$$

The negative signs for $\Delta\sigma_T$ and $\Delta\sigma_L$ in (2.5) and (2.6) correspond to the usual, although unjustified, convention in the literature. The total cross section differences are measured with either parallel or antiparallel beam and target polarization directions. Polarization vectors are transversally oriented with respect to $\mathbf{k}$ for $\Delta\sigma_T$ measurements and longitudinaly oriented for $\Delta\sigma_L$ experiments.

The total cross section differences $\Delta\sigma_T$ and $\Delta\sigma_L$ are deduced from four total cross section measurements, respectively. General expressions for $\Delta\sigma_T$ are given in [18]; here we give relations for $\Delta\sigma_L$:

$$\sigma(\rightrightarrows) = \sigma_{0\text{tot}} + |P_B^+ P_T^+|(\sigma_{1\text{tot}} + \sigma_{2\text{tot}}), \tag{2.7a}$$

$$\sigma(\leftrightarrows) = \sigma_{0\text{tot}} - |P_B^- P_T^+|(\sigma_{1\text{tot}} + \sigma_{2\text{tot}}), \tag{2.7b}$$

$$\sigma(\rightleftarrows) = \sigma_{0\text{tot}} - |P_B^+ P_T^-|(\sigma_{1\text{tot}} + \sigma_{2\text{tot}}), \tag{2.7c}$$

$$\sigma(\leftleftarrows) = \sigma_{0\text{tot}} + |P_B^- P_T^-|(\sigma_{1\text{tot}} + \sigma_{2\text{tot}}). \tag{2.7d}$$

Since the beam polarization direction at the Synchrophasotron could be reversed at every cycle of the accelerator, it is preferable to calculate $\Delta\sigma_L$ from pairs of $|P_B^+|$ and $|P_B^-|$ measurements with the same target polarization. Values of $|P_T^+|$ and $|P_T^-|$ are well known as a function of time. The spin-independent term drops out when taking the difference, and one obtains:

$$-\Delta\sigma_L(P_T^+) = 2(\sigma_{1\text{tot}} + \sigma_{2\text{tot}})^+ = \frac{2[\sigma(\rightrightarrows) - \sigma(\leftrightarrows)]}{(|P_B^+| + |P_B^-|)|P_T^+|}, \tag{2.8a}$$

and

$$-\Delta\sigma_L(P_T^-) = 2(\sigma_{1\text{tot}} + \sigma_{2\text{tot}})^- = \frac{2[\sigma(\leftleftarrows) - \sigma(\rightleftarrows)]}{(|P_B^+| + |P_B^-|)|P_T^-|}, \tag{2.8b}$$

with beam and target polarized along **k**. The asymmetry, proportional to the arithmetic average

$$P_B = |P_B| = \tfrac{1}{2}(|P_B^+| + |P_B^-|) \tag{2.9}$$

is continuously measured by beam polarimeters. One can see that an unpolarized beam is not necessary for $\Delta\sigma_{L,T}$ measurements.

Possible effects of a counter misalignment and perpendicular components in the beam (or target) polarization cancel out, giving the final results as a simple (unweighted) average

$$\Delta\sigma_L = \tfrac{1}{2}[\Delta\sigma_L(P_T^+) + \Delta\sigma_L(P_T^-)]. \tag{2.10}$$

Putting (2.8a) and (2.8b) into (2.10) we have

$$\Delta\sigma_L = \frac{1}{|P_B^+| + |P_B^-|}\left(\frac{\sigma(\rightrightarrows) - \sigma(\leftrightarrows)}{|P_T^+|} + \frac{\sigma(\leftleftarrows) - \sigma(\rightleftarrows)}{|P_T^-|}\right). \tag{2.11}$$

More details are given in [4, 18].

3 Polarized beam

Polarized neutrons and protons were produced by break-up of accelerated vector-polarized deuterons [1] on a target of 17 cm beryllium and 6 cm of carbon. The kinetic energy of accelerated deuteron decreases by 3 MeV by passage in air and then by 17 MeV by absorption in the half of the target thickness. The total losses of (20 ± 17) MeV are practically the same at all measured energies and must be subtracted from the nominal accelerator values. The neutron mean energy is then one half of the deuteron energy in the center of the production target. The neutron momentum distribution in the forward break-up reaction, due to the Fermi motion of the nucleons in accelerated deuterons has a gaussian-like shape with FWHM ~5% of neutron momentum.

The production target was positioned close to one focal point of the deuteron beam line. Protons and deuterons were removed from the neutron beam by a bending magnet. The deuteron beam intensity was continuously monitored by two calibrated ionization chambers in front of the target. Neutrons were collimated by 6 m iron and brass in a path of 7 m upstream from the transmission set-up. The neutron angular divergence was ~1.5 mrad. The collimators and efficient shielding of the experimental area decreased the low energy tail of the neutron spectrum to about 1%.

The neutron beam spot at the PPT was 28 mm in diameter. This spot was monitored using charge exchange particles produced in a radiator of a proportional chamber downstream from the PPT. The number of neutrons was determined in dedicated measurements by an activation method. The deuteron beam intensities and corresponding neutron fluxes at the PPT, averaged over the data acquisition, are listed in Table 1.

The neutron intensity decreases with decreasing neutron momentum $p_{\mathrm{lab}}(n)$ since the neutron emission solid angle increases as a function of $1/[p_{\mathrm{lab}}(n)]^2$. From Table 1 follows that the intensity decreases more rapidly due to a degradation of the beam extraction efficiency at lower energies.

Table 1. Averaged deuteron beam intensities and neutron fluxes at three energies

$T_{\mathrm{kin}}(d)$ (GeV) accelerator	$T_{\mathrm{kin}}(d)$ (GeV) target center	$T_{\mathrm{kin}}(n)$ (GeV) mean	Deuterons per spill	Neutrons per spill (PPT)
2.40	2.38	1.19	5.3×10^8	2.7×10^4
5.00	4.98	2.49	6.1×10^8	2.0×10^5
7.32	7.30	3.65	6.4×10^8	4.7×10^5

The repetition time of the Synchrophasotron was 8 to 10, depending on energy, and the spill length was typically 0.5 s. The deuteron beam polarization direction was flipped every spill of the accelerator.

The polarization of incident deuterons $\mathbf{P}_B(d)$ was oriented perpendicularly with respect to the beam momentum, along the vertical axis. The polarization of the produced neutrons $\mathbf{P}_B(n)$ had the same direction. The neutron polarization was rotated to the longitudinal direction by a spin rotation dipole with the maximum horizontal field integral of 2.7 Tm. The spin rotator was positioned in front of the PPT and removed a considerable fraction of the protons produced in collimators. The beam line allowed to extract the low intensity deuteron beam towards the experimental area and check the beam alignment and bending of deuterons in the spin rotator. This procedure checks the signs of the $\Delta\sigma_L$ results.

The absolute polarization of deuterons was deduced from the asymmetry measurement of $dp \Rightarrow dp$ elastic scattering. For this reason the deuteron beam was periodically deviated into another beam line towards the two-arm magnetic spectrometer ALPHA [19]. The deuteron beam momentum was set to 3.0 GeV/c where the analyzing power is well known from the SATURNE II measurements [20]. Deuterons were scattered in the liquid hydrogen target, forward deuterons and recoil protons were detected in two pairs of kinematically conjugate arms at $\theta_{\mathrm{lab}}(d) = 7.45^\circ$. This angle is close to a maximum vector analyzing power. The magnetic analysis of forward deuterons removed inelastic events [19]. The measurement provided the $P_B(d)$ value, directly related to the neutron beam polarization $P_B(n)$. The result yields the mean value for "up" and "down" neutron beam polarization $|P_B(n)| = 0.535 \pm 0.009$.

No depolarizing resonances of the internal deuteron beam in the synchrophasotron exist up to the highest accelerator energy. This has been determined over the entire energy range [19] using a beam decceleration method described in [21]. Consequently, it was sufficient to determine the deuteron beam polarization at one energy only.

A direct absolute measurement of the neutron beam polarization has not been performed during the run. The $P_B(n)$ could have been determined e.g. by a comparison of the beam and target analyzing powers, $A_{oono}(np)$ and $A_{ooon}(np)$, respectively [15], assuming that the target polarization P_T is known [22].

The stability of the $P_B(d)$ value was continuously monitored by another beam polarimeter [23], measuring

Table 2. Mean values of the quasielastic *pp* asymmetry at four proton energies

$T_{kin}(p)$ (GeV)	$p_{lab}(p)$ (GeV/c)	θ_{lab} (deg)	θ_{CM} (deg)	$\varepsilon(pp)$
0.83	1.50	14	33.3	0.246 ± 0.016
1.20	1.92	14	35.4	0.2214 ± 0.0015
2.50	3.31	8	24.2	0.1434 ± 0.0015
3.66	4.50	8	27.1	0.0807 ± 0.0020

Table 3. Characteristics of the MPT

Target length (mm) [20°C]	Target diameter (mm) [20°C]	Container volume (cm^3) [20°C]	Sample weight (g) [70 K]	Filling factor
200.0 ± 0.1	30.0 ± 0.1	141.37 ± 0.95	95.5 ± 0.3	0.67

quasielastic scattering of bounded protons in accelerated deuterons on a CH_2 target. This polarimeter consists of two pairs of arms, each of them equipped with two scintillation counters. Both pairs of arms were positioned at $pp \Rightarrow pp$ kinematically conjugate angles and measured the left-right asymmetry $\varepsilon(pp)$. The angle was close to the forward maximum of the *pp* elastic scattering analyzing power A_{oono}. The measurement showed the excellent stability of $\varepsilon(pp)$ during data taking. The results of individual runs show that the dispersion of $\Delta\varepsilon(pp)$ was smaller than ± 0.005 for each energy. The mean values of $\varepsilon(pp)$ at four proton energies (including data at the deuteron beam momentum 3 GeV/c) are given in Table 2.

4 Polarized proton target

The Dubna target for the present experiment contains main parts of the Saclay-Argonne frozen spin proton polarized target, used initially in the E704 experiment at FERMILAB (USA) [24, 25]. The target has been reassembled and upgraded adding the missing parts for the purposes of the Dubna physics program. With respect to the FERMILAB experiment a concept of a "movable polarized target" (MPT) has been applied [26]. It consists in a transportability of the target from one experimental area to another. All the major parts of the target assembly located close to the beam line were mounted on two separate decks, which can be moved as units in and out of the beam, even when the target is polarized.

The largest of the two movable decks contains the $^3He/^4He$ horizontal dilution refrigerator mounted on a 1.5 ton concrete cube, a 30 ℓ service helium dewar of the refrigerator, a 1000 ℓ supply helium dewar, the ^3He pumping system, the NMR system and a microwave generator. These last two items are used for dynamic nuclear polarization measurement and build-up. The quality of the vibrational insulation was demonstrated by the fact that it was possible to work in the frozen polarization mode at a working temperature of 50 mK without any additional thermal load to the refrigerator, and only a negligible phonic noise on the NMR coils was observed.

A polarizing superconducting solenoid, its 300 ℓ service helium dewar and power supplies are mounted on the smaller deck. For easier operation and for a free access to detectors, the target equipment not mounted on the decks is placed outside of the radiation controlled area.

Remote control of the entire operation of the MPT consisted of the ^3He and ^4He control panels, an interlock system, and controls for the NMR and microwave systems. A new powerful two-arm cleaning system for ^3He was built (warm silicagel traps and charcoal traps cooled by liquid nitrogen).

The target material used in the experiment was 1,2-propanediol $C_3H_6(OH)_2$ with a paramagnetic Cr^V impurity, having a spin concentration of 1.5×10^{20} cm^{-3} [27]. The propanediol beads were loaded in a hydrogen-free container placed inside the dilution refrigerator. The PPT contains $(8.93 \pm 0.27).10^{23}/cm^{-2}$ polarized hydrogen atoms. The target characteristics at the room temperature and at the temperature of liquid nitrogen (70 K) are given in Table 3.

The target polarization measurements were carried out using a computer controlled NMR system. Maximum values of proton polarization obtained were 0.842 and -0.906 for positive and negative polarizations, respectively. The difference of microwave frequencies corresponding to polarization maxima was measured to be 340 MHz. The duration of one continuous run at a given sign of target polarization was about 12 hours. The polarization degradation during this period was insignificant since the nuclear spin relaxation time in the frozen spin mode (at a temperature 50 mK and magnetic field 2.69 T) was over 1000 hours.

For further experiments a transverse polarization of protons (and deuterons) is foreseen and a set of transverse holding coils is under construction.

5 Transmission detectors set-up and electronics

The experimental set-up is shown in Fig. 1. The hardware used was described in detail in [2, 3]; here we give only the most important items. The setup consisted of 5 independent units, two of them are used as beam monitors (S_i), and the three remaining ones as transmission detectors (T_j). The units were of similar design and the electronics were identical. We can discuss only one pair of S_i and T_j ($i = 1, 2$ and $j = 1, 2, 3$). Each unit consisted of a CH_2 converter placed behind a large veto scintillation counter S3A (T3A). Charged particles emitted forward were detected by two counters S1 and S2 (T1 and T2) in coincidence. The monitor converters and S1, 2 counters were 30 mm in diameter and the corresponding elements of the transmission detectors were 90 mm. It has been measured that with increasing radiator thickness, the detector efficiency first increases, reaches a broad maximum at about 60–80 mm, and then starts to decrease slowly. For this reason the thickness of all converters was set to 60 mm. The transmission detectors, each close to the other were positioned 6 meters downstream from the target center.

The electronics of one *S* unit is shown in Fig. 2.

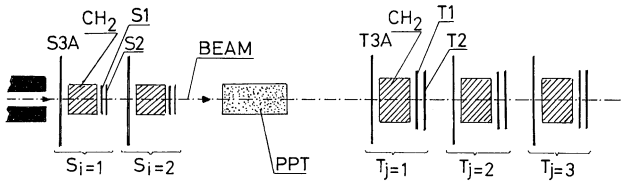

Fig. 1. Experimental set-up for the $\Delta\sigma_L(np)$ measurements. $S1$, $S2$, $S3A$, $T1$, $T2$ and $T3A$ are scintillation counters, and CH_2 are radiators

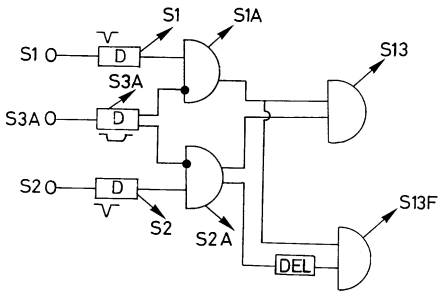

Fig. 2. Electronic diagram of the monitor detectors. D are discriminators, and arrows denote the scalers

The following rates were recorded for each spill of the accelerator:

$S13 = (S1.\overline{S3A}).(S2.\overline{S3A})$,

$T13 = (T1.\overline{T3A}).(T2.\overline{T3A})$,

$S1A = (S1.\overline{S3A})$,

$S2A = (S2.\overline{T3A})$,

$T1A = (T1.\overline{T3A})$,

$T2A = (T2.\overline{T3A})$,

as well as accidental coincidences:

$S13F = S1A.S2A$(delayed),

$T13F = T1A.T2A$(delayed)

and single counts in each of the six counters. These data were recorded for each unit S_i and T_j by scalers, and were read by the computer after the end of every spill. A necessary statistics for this type of experiment can only be obtained from scalers rates, rather then individual events written on tape.

6 Data acquisition and experimental errors

If N_{in} is the number of neutrons incident on the target and N_{out} the number of neutrons transmitted in a counter array of solid angle Ω, then the total cross section is:

$$N_{\text{out}} = N_{\text{in}} \exp[-\sigma(\Omega) n_H x], \tag{6.1}$$

where n_H is the number of oriented hydrogen atoms per cm^3 and x is the target thickness. $\sigma(\Omega)$ depends on the polarizations $P_B^{\pm}$ and $P_T^{\pm}$ as shown in (2.7a, b, c, d). If one sums over the events taken with fixed target polarization P_T^+ and P_T^- as shown in Eqs (2.7a, b, c, d) and using (2.8a) or (2.8b), the ratio of the measurements with the beam polarization P_B from (2.9) becomes:

$$R^{\pm} = \frac{(N_{\text{out}}/N_{\text{in}})^-}{(N_{\text{out}}/N_{\text{in}})^+} = \exp[\Delta\sigma(\Omega)\ P_B P_T^{\pm} n_H x] \tag{6.2}$$

for either target polarization $P_T^{\pm}$.

Because $N_{\text{out}} = T/\eta(T)$ and $N_{\text{in}} = S/\eta(S)$ where $T = T13 - T13F$ ($S = S13 - S13F$) is the number of neutrons seen in the T (S) detector and $\eta(T)$ ($\eta(S)$) its efficiency, we get:

$$R(P_T^{\pm}) = \frac{[T/S](P_B^-)}{[T/S](P_B^+)} \tag{6.3}$$

and

$$\Delta\sigma_L(\Omega, P_T^{\pm}) = \frac{1}{P_B.P_T^{\pm}.n_H.x} \ln R(P_T^{\pm}). \tag{6.4}$$

As can be seen from (6.4) the statistical error of $\Delta\sigma_L$ decreases linearly with increasing x. Uncertainties in a determination of P_B, P_T and $n_H.x$ are normalization errors which move all results up or down independent of energy. We estimate the relative errors $\Delta P_B/P_B = \pm 2.3\%$, $\Delta P_T/P_T = \pm 3.0\%$ and $\Delta(n_H.x)/(n_H.x) = 3.1\%$, including the uncertainty of the filling factor and a possible error of the target temperature measurement. The spin rotator field setting and its inhomogeneity may provide an additional systematic error of $\pm 1.1\%$, which is constant during measurements at one energy only.

All the formulae in Sect. 2 were deduced for a pure polarized hydrogen target. The presence of carbon and oxygen in the PPT beads add terms $\sigma_{\text{tot}}(C)$ in (2.7). These terms are spin-independent, since ^{12}C has no spin and therefore its contribution drops out in differences (2.8). The same occurs for ^{16}O and ^{4}He in the target. However, there are negligibly small contributions from ^{13}C and ^{3}He, which may be slightly polarized. This uncertainty was estimated to be 0.5%. No spin-dependent effect from the teflon container for the Saclay target [28] in working conditions has been observed. The ratio of polarized hydrogen to other target nuclei depends on the target material, and is fairly independent of target size.

Since a transmission spin effect manifests itself in the presence of polarized beam and target only, no contribution to $\Delta\sigma$ occurs if some beam neutrons miss the PPT. This will increase the spin-independent term, subtracted in differences.

The extrapolation of $\Delta\sigma_L(\Omega)$ towards zero solid angle gives $\Delta\sigma_L$. The maximal solid angle subtended by each of the three T detectors from the center of the MPT was about $\Omega_{\text{lab}} = 3.44 \times 10^{-4}$ sr i.e. $\theta_{\text{lab}} = 0.6^\circ$. The laboratory angle corresponds to $\theta_{CM} = 1.54^\circ$, 1.83° and 2.06° at 1.20, 2.50 and 3.66 GeV, respectively. The angles are small enough that the extrapolation of results towards $\Omega = 0$ is

not necessary. In our energy range the difference between the measured value and the value extrapolated to $\Omega = 0$ is expected to be smaller than at SATURNE II energies, where it has been estimated to be less than 0.05 mb. This is much smaller than the statistical error in the present experiment.

The neutron detection efficiencies of about 2% for all detectors are practically constant with energy. The efficiencies were determined with respect to a calibrated ionization chamber in front of the production target.

The counter array used provides very good stability of the detection efficiency. Note that the results depend neither on the absolute efficiencies of S_i and T_j, nor on their ratio (6.3). The small detection efficiencies decrease the probability for a converted neutron to be accompanied by another quasi-simultaneous converted neutron in the same detector. The "simultaneous" detection is to be understood within the resolution time of a plastic scintillation counter (20 ns). This probability was estimated from results obtained with different neutron beam intensities and radiator thicknesses [3, 4]. For the same neutron fluxes, it increases quadratically with increasing $\eta_{S,T}$. For high counter efficiencies (namely for *pp* transmission experiments) it represents the dominant source of systematic errors. At SATURNE II the neutron counter efficiences were of the same order, the neutron beam intensity was around 7.10^7/spill (hundred times more) and the spill length was compatible with that of the Synchrophasotron. The simultaneous conversion probability has been found to be always smaller than 10^{-4}, corresponding to a maximum systematic error of ± 0.25 mb at Saclay. It was estimated to be negligible in the present experiment.

Possible misalignment of the detector components or the entire detectors provide left-right (up-down) instrumental asymmetries. The asymmetries in each S_i and T_j detector will depend on the transverse beam polarization components (P_{Bn} and P_{Bs}) only. For T_j detectors they are practically independent of the target polarization [3,18]. This asymmetry $\varepsilon_{Bn}(instrum)$ may be of the same order or larger than the transmission effects, even for a small counter and radiator misalignment. The $\varepsilon_{Bn}(instrum)$ provides the same contributions to each pair of measurements in (2.7a, b) and (2.7c, d) and it cancels out when taking the simple average of results in (6.4). Since the present experiment uses almost longitudinal beam, the displacement effects for $\Delta\sigma_L$ can be neglected.

The distribution of results from independent measurements for the same sign of the target polarization show that fluctuations were about 1.005 times larger than expected from statistics alone. We have added quadratically an error of $\pm 0.5\%$ for random-like instrumental effects.

A possible inefficiency of the protection against charged particles (veto counters $S3A$ and $T3A$) may exist. Charged particles in the neutron beam are produced mainly in beam collimators, in CH_2 radiators of all S_i and T_j detectors, and in the target. Only a small fraction of the forward protons is polarized. They are produced in the polarized target by elastic scattering of polarized neutrons on free polarized protons close to $\theta_{CM} = 180^\circ$. For the longitudinally polarized beam and target one obtains a contribution from the spin correlation parameter $A_{ookk}(np)$, which is included in the counting rate asymmetry for the observable $\Delta\sigma_L$. The A_{ookk} spin correlation has been measured at 1.10 GeV where its value at 178.7° CM reaches -0.53 ± 0.01 [29]. This observable shows a rapid decrease towards large negative values as a function of scattering angle. This could be seen in Table 4 where predictions for $A_{ookk}(np)$ close to 180° CM [30] together with measured *np* differential cross sections in the backward direction are listed.

In the present experiment at 1.19 GeV within the laboratory solid angle $\Delta\Omega(\text{lab}) = 3.44 \times 10^{-4}$sr (i.e. $\Delta\Omega(CM) = 2.27 \times 10^{-3}$sr) and with the flux of 10^5 neutrons/spill, one obtains less than 1 scatter/spill. This corresponds to an additional asymmetry of 10^{-4} for completely inefficient veto counters. From Table 4 it follows that the spin correlation parameter contribution $A_{ookk}(np)$ moves $-\Delta\sigma_L(np)$ towards negative values. Since the efficiencies of veto counters are better than 98% the additional asymmetry will decrease to 2.10^{-6} and may provide a $\pm 0.1\%$ systematic error. The $A_{ookk}(180^\circ)$ CM observable represents one of parameters which determine the real parts of scattering amplitudes for the isospin $I = 0$ state. A measurement of this observable at 180° CM is foreseen in the future.

Other checks were performed in order to estimate the target effects. Measurements were carried out with an empty polarized target, with the target removed from the solenoid and without any target element in the neutron beam line. Results of these tests are listed in Table 5. All transmission ratio results are in excellent agreement with calculated values.

In Table 6 is given a summary of the maximal contributions to $\Delta\sigma_L(np)$ from different sources of systematic uncertainties. The total systematic error is then $\pm 5\%$ of the measured value. The absolute error of ± 0.05 mb due to the extrapolation towards zero solid angle is to be added.

Table 4. Existing data for *np* differential cross sections and predictions for $A_{ookk}(np)$ close to 180° CM at several energies

$T_{kin}(n)$ (GeV)	$(d\sigma/d\Omega)$ (180°) (mb)	A_{ookk} 170°CM	A_{ookk} 175°CM	A_{ookk} 180°CM
0.80	8.14 ± 0.19	-0.549	-0.864	-0.911
0.90	8.70 ± 0.62	-0.472	-0.840	-0.899
1.00	8.70 ± 0.27	-0.409	-0.828	-0.897
1.10	9.11 ± 0.27	-0.360	-0.825	-0.903
1.20	7.32 ± 0.25	-0.329	-0.832	-0.916
1.30	5.30 ± 0.35	-0.317	-0.846	-0.933
2.50	3.00 ± 0.30			
4.15	2.26 ± 0.24			

Table 5. Transmission measurements for different MPT configurations

MPT configuration	Transmission ratio
MPT absent	1.000
MPT solenoid istalled only	0.994
MPT without the propanediol sample	0.936
MPT operationnel	0.729

Table 6. Summary of systematic uncertainties

Origin of the uncertainty	Contribution ± to $\Delta\sigma_L(np)$ (%)
Beam polarization	2.3
Target polarization	3.0
Number of polarized target H-atoms	3.1
Neutron spin rotator	1.1
Polarization of other atoms	0.3
Inefficiencies of veto counters	0.1
Random-like instrumental effects	0.5

7 Results and discussion

All combinations of the two monitors $S_{1,2}$ and three transmission detectors $T_{1,2,3}$ counting rates were taken into account. They provided a check of the compatibility of the results. The final results for this experiment were deduced from measured rates $\sum_i S_i$ and $\sum_j T_j$ for corresponding beam and target polarization configurations. They are listed in Table 7. The errors of the present results contain statistical and systematic errors added in quadrature. Results are shown in Fig. 3 together with existing data [3, 4, 6, 8, 9] measured with free polarized neutrons. All data smoothly connect in the entire energy region. The solid curve was calculated by the energy dependent phase shift analysis [30] where the present results were not introduced. We observe a fast decrease in the $-\Delta\sigma_L(np)$ energy dependence. This seems to be in disagreement with the PSA predictions, but no extrapolation is allowed out of the region of existing data.

In Fig. 4, the curve 1 represents the energy dependence of $-\Delta\sigma_L(np)$ observable, measured with the free polarized neutron beams above 0.4 GeV. This curve is compared with the difference between $-\Delta\sigma_L(dp)$ and $-\Delta\sigma_L(pp)$ results obtained at the ANL-ZGS [13]. We observe a good agreement above 1 GeV and a confirmation of the $-\Delta\sigma_L(np)$ behaviour, discussed above.

The similar quantity in pp transmission, $\Delta\sigma_L(pp)$, also decreases with energy [2] and tends to zero. This is in agreement with the prediction of a nonperturbative QCD model for spin effects, treated in [31]. The model predicts that the quark interaction induced by strong fluctuations of vacuum gluon fields, i.e. instantons [32], provides the large contribution to the $\Delta\sigma_L$ observable [33]. Important features of this interaction are its spin and flavor dependence. The interaction cannot vanish only for the quarks which have the same helicity but a different flavor. The maximal instanton contribution to the $-\Delta\sigma_L(np)$ is shown in Fig. 4 by the dot-dashed curve (2). Two minima were predicted for instanton-induced contribution: one close the two-pion production threshold (a), second one at the $(2\pi + \eta)$ threshold (b). The model can explain qualitatively the observed $\Delta\sigma_L$ energy dependence for np as well as for pp transmission.

It will be very interesting to measure the total cross section difference $\Delta\sigma_T(np)$, using the tranversely polarized beam and target. This quantity may show a different behavior at high energies, according to a prediction of this model.

Table 7. $-\Delta\sigma_L(np)$, $-\Delta\sigma_L(pp)$ and $-\Delta\sigma_L(I=0)$ data.

$T_{kin}(n)$ (GeV)	$-\Delta\sigma_L(np)$ (mb)	$-\Delta\sigma_L(pp)$ (mb)	$-\Delta\sigma_L(I=0)$ (mb)
1.19	7.10 ± 3.70	9.98 ± 0.25	4.22 ± 7.40
2.49	-0.85 ± 1.32	2.02 ± 0.29	-3.72 ± 2.64
3.65	0.30 ± 0.84	1.74 ± 0.04	-1.14 ± 1.68

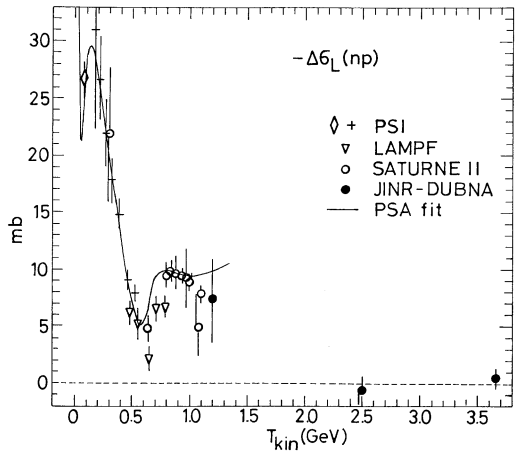

Fig. 3. Energy dependence of $\Delta\sigma_L(np)$. Meaning of the symbols: ● ..... present experiment, diamond ..... PSI, [9], + ... PSI, [6], ▽ ..... LAMPF, [8], ○ ..... SATURNE II, [3, 4], solid line ..... PSA, [30]

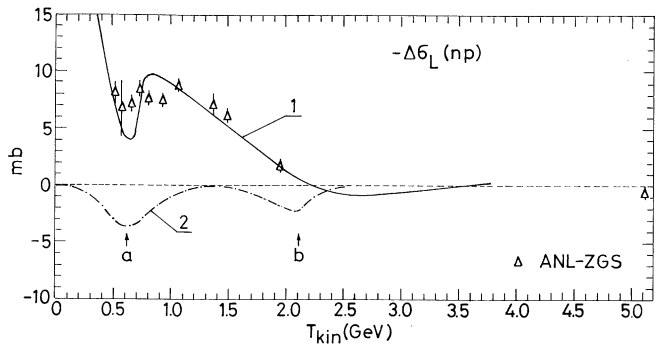

Fig. 4. The solid curve 1 represents the energy dependence of $-\Delta\sigma_L(np)$ observable, measured with the free polarized neutron beams above 0.4 GeV. This curve is compared with the difference between $-\Delta\sigma_L(dp)$ and $-\Delta\sigma_L(pp)$ results obtained at the ANL-ZGS [13] (△). The maximal instanton contribution to the $-\Delta\sigma_L(np)$ is shown by the dot-dashed curve 2. Two minima were predicted for instanton-induced contribution [33]: one close the two-pion production threshold (a), second one at the $(2\pi + \eta)$ threshold (b)

The lowest lying exotic quark configurations in the isospin state $I = 1$ and the spin-singlet state $^1S_0$ with the mass of 2.7 GeV ($T_{kin}(p) = 2.1$ GeV) was predicted by Lomon et al. [34–38]. The authors used the Cloudy Bag Model and an R-matrix connection to long range meson exchange forces. Their prediction is in qualitative agreement with Resonating Group Method calculations for constituent quark models (CQM), as predicted by Wong [39] for the relativistic CQM, and by Kalashnikova et al. [40] for the non-relativistic CQM.

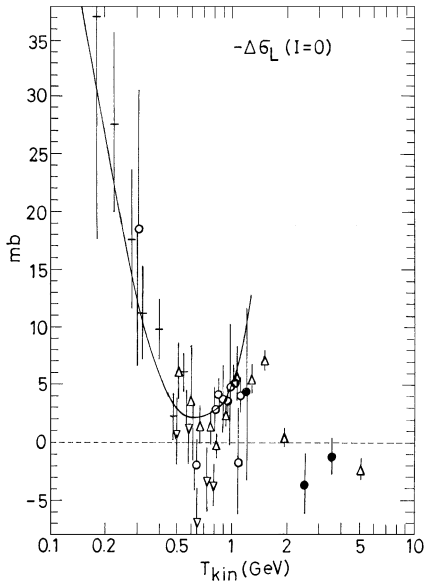

Fig. 5. Energy dependence of $\Delta\sigma_L(I=0)$. The *np* data plotted in Figs. 3 and 4 were used (the present symbols have the same meaning). The *pp* data were calculated from the Saclay-Geneva PSA [50, 51] for *np* results from [3, 4, 6, 8]. ANL-ZGS $I=0$ data are given by authors of [13]. At 1.19 and 2.49 GeV *pp* data were taken as average values from ANL-ZGS and SATURNE II measurements [3, 4, 13]. At 3.65 GeV interpolated *pp* values from ANL-ZGS were used

A resonance-like structure has been suggested by the energy dependence of the $\Delta\sigma_L(pp)$ [2,41], as well as by the measurement of the spin correlation parameter $A_{oonn}(pp)$ at 90°CM [42]. Other indications can be found in [43–48]. The present data allow no conclusions yet and new measurements with smaller steps in energy throughout the region from 1.5 to 4.0 GeV are highly desirable.

The $\Delta\sigma_L$ observables measured in the *np* and *pp* transmission at the same energy are related with the quantity for the isospin $I=0$ state [2]. It holds:

$$\Delta\sigma_L(I=0) = 2\Delta\sigma_L(np) - \Delta\sigma_L(pp). \tag{7.1}$$

Using (7.1) and existing *np* and *pp* data one deduces $\Delta\sigma_L$ values for $I=0$. Since the *pp* data are very accurate, the $I=0$ values will have roughly two times larger errors than *np* data.

In order to deduce $\Delta\sigma_L(I=0)$ values from the present measurements, the averaged values of the $\Delta\sigma_L(pp)$ data measured at SATURNE II and at the ANL-ZGS were used (see [2] and references therein). The results are given in Table 7 and plotted in Fig. 5, together with the PSA predictions from [30] and the values deduced from PSI, LAMPF, ANL-ZGS and Saclay *np* measurements.

The $-\Delta\sigma_L(I=0)$ value sharply increase towards low energy (at 66 MeV $-\Delta\sigma_L(I=0) = (88.6 \pm 4.0)$ mb). At high energies we observe an unexpected although well pronounced maximum somewhere above 1.5 GeV, followed by a rapid decrease with increasing energy. It means that $-2\Delta\sigma_L(np)$ decreases faster then $-\Delta\sigma_L(pp)$ in this energy range. This behaviour is also in qualitative agreement with the instanton model. It supports more strongly the prediction of [49], concerning a position ot the lowest lying exotic quark configuration for isospin $I=0$ in the spin-triplet wave $^3S_1$ at a mass 2.63 GeV ($T_{\rm kin}(n) = 1.8$ GeV). In the $\Delta\sigma_L(I=0)$ the spin-singet partial wave $^1S_0$ ($I=1$) is absent and the $^3S_1$ wave ($I=0$) may be predominant. To confirm this observation a measurement of $\Delta\sigma_T(np)$ is needed in order to deduce $\Delta\sigma_T(I=0)$. In the last quantity the uncoupled spin-triplet is absent and the coupled spin-triplet amplitude is expected to be less diluted.

8 Conclusions

The present results increase the energy range of existing $\Delta\sigma_L(np)$ data up to 3.65 GeV. The Dubna results connect smoothly with the Saclay free *np* measurements and are in excellent agreement with the *pn* quasielastic ANL-ZGS data. They are compared with existing models and with the predictions of the phase shift analysis. Using the present *np* results and the existing *pp* data measured at SATURNE II and at ANL-ZGS, the $\Delta\sigma_L$ values for the isospin state $I=0$ were obtained. They show a well pronounced sharp maximum above 1.5 GeV. Our results will improve spin-dependent dispersion-relation calculations as well as the existing PSA solutions. The data can also be used to check theoretical models.

Acknowledgements. We acknowledge support for this work from J. Arvieux, A.M. Baldin, P. Borgeaud, F. Bradamante, V.P. Dzhelepov, J.Haïssinski, I.M. Karnaukhov, Ph.Leconte, Yu.C. Oganesian, V.A. Matveev, B. Peyaud, V.S. Rumyantsev, N.A. Russakovich, I.A. Savin, A.N. Sissakian, J.J. de Swart and H. Walter. Discussions with J. Bystricky, P. Chaumette, J. Derégel, A.E. Dorokhov, M. Finger, M. Giorgi, R. Hess, Z. Janout, Yu.F. Kisselev, R. Kunne, C. Lechanoine-Leluc, S. Mango, B.S. Neganov, S. Pospíšil, D. Rapin, M.P. Rekalo, I.I. Strakovsky, I. Wilhelm, and C. Wilkin have solved several problems. We thank the accelerator crew and N.N. Agapov with the staff of the liquid helium plant as well as the LNP and LHE JINR workshop staff for efficient help. The exploitation of the polarized target owes a lot to A.V. Gevchuk and R.L. Khamidulin. We acknowledge contributions of T.B. Ivashkevich, Z.P. Motina, V.M. Zhabitsky and P.I. Zarubin to organization of the experiment. This work was partly supported by the International Association for the Promotion of Cooperation with Scientists from the Independent States of the Former Soviet Union (INTAS) grant No 93-3315, by the Russian Foundation for Basic Research grants RFBR-93-02-03961, RFBR-93-02-16715 and RFBR-95-02-05807, by the International Science Foundation and Russian Government grant No. JWH 100, and by the US Department of Energy Contract No. W-31-109-ENG-38.

References

1. I.B. Issinsky, A.D. Kirillov, A.D. Kovalenko and P.A. Rukoyatkin, Acta Physica Polonica B25 (1994) 673
2. C. Lechanoine-Leluc and F.Lehar, Rev. Mod. Phys. 65 (1993) 47
3. F. Lehar, A. de Lesquen, L. van Rossum, P. Chaumette, J. Derégel, J. Fabre, M. de Mali, J.M. Fontaine, D. Legrand, F. Perrot, J. Ball, C.D. Lac, P. Bach, G. Gaillard, R. Hess, Ph. Sormani, V. Ghazikhanian, C.A. Whitten, R. Peschina, E. Rössle, Phys. Lett. 189B (1987) 241
4. J.M. Fontaine, F. Perrot-Kunne, J. Bystricky, J. Derégel, F. Lehar, A. de Lesquen, M. de Mali, L. van Rossum, J. Ball, Ph.

Chesny, C.D. Lac, J.L. Sans, J.P. Goudour, P. Bach, G. Gaillard, R. Hess, R. Kunne, D. Rapin, Ph. Sormani, R. Binz, A. Klett, R. Peschina, E. Rössle, H. Schmitt, Nucl. Phys. B358 (1991) 297
5. J. Ball, Ph. Chesny, M. Combet, J.M. Fontaine, R. Kunne, M.C. Lemaire, J.L. Sans, J. Bystricky, F. Lehar, A. de Lesquen, M. de Mali, F. Perrot-Kunne, Ph. Demierre, G. Gaillard, R. Hess, D. Rapin, L.S. Barabash, Z. Janout, B.A. Khachaturov, Yu.A. Usov, D. Lopiano, H. Spinka, R. Binz, A. Klett, E. Rössle, H. Schmitt, Zeit. Phys. C61 (1994) 53
6. R. Binz, B. van den Brandt, R. Büchle, M. Daum, Ph. Demierre, J. Franz, G. Gaillard, N. Hamann, R. Hess, J.A. Konter, F. Lehar, C. Lechanoine-Leluc, S. Mango, R. Peschina, F. Perrot-Kunne, D. Rapin, E. Rössle, P.A. Schmelzbach, H. Schmitt and R. Todenhagen, Nucl. Phys. A533 (1991) 601
7. R. Binz, R. Büchle, M. Daum, J. Franz, G. Gaillard, N. Hamann, R. Hess, S. Jaccard, F. Lehar, C. Lechanoine-Leluc, A.C. Letestu, R. Peschina, D. Rapin, E. Rössle, P.A. Schmelzbach, H. Schmitt, R. Todenhagen, and H.L. Woolverton, Phys. Lett. B231 (1989) 323
8. M. Beddo, G. Burleson, J.A. Faucett, S. Gardiner, G. Kyle, R. Garnett, D.P. Grosnick, D. Hill, K.F. Johnson, D. Lopiano, Y. Ohashi, T. Shima, H. Spinka, R. Stanek, D. Underwood, A. Yokosawa, G. Glass, R. Kenefick, S. Nath, L. Northcliffe, J.J. Jarmer, S. Penttila, R.H. Jeppesen, G. Trippard, M. Devereux and P. Kroll, Phys. Lett. 258B (1991) 24
9. P. Hafner, C. Brogli-Gysin, J. Campbell, D. Fritschi, J. Götz, M. Hammans, R. Henneck, J. Jourdan, G. Masson, L.M. Quin, S. Robinson, I. Sick, M. Tucillo, J.A. Konter, S. Mango and B. van den Brandt, Nucl. Phys. A548 (1992) 29
10. W.S. Wilburn, C.R. Gould, D.G. Haase, P.R. Huffman, C.D. Keith, J.E. Koster, N.R. Roberson and W. Tornow, Phys. Rev. Lett. 71 (1993) 1982
11. W.S. Wilburn, C.R. Gould, D.G. Haase, P.R. Huffman, C.D. Keith, N.R. Roberson and W. Tornow, Phys. Rev. C52 (1995) 2353
12. J. Brož, J. Černý, Z. Doležal, G.M. Gurevich, M. Jirásek,. P. Kubík, A.A. Lukhanin, J. Švejda, I. Wilhelm, N.S. Borisov, Yu.M. Kazarinov, B.A. Khachaturov, E.S. Kuzmin, V.N. Matafonov, A.B. Neganov, I.L. Pisarev, Yu.A. Plis, Yu.A. Usov, M. Rotter and B. Sedlák, Zeit. Phys. A, to be published 1996
13. I.P. Auer, W.R. Ditzler, D. Hill, H. Spinka, N. Tamura, G. Theodosiou, K. Toshioka, D. Underwood, R. Wagner, and A. Yokosawa, Phys. Rev. Lett. 46 (1981) 1177
14. W. Grein and P. Kroll, Nucl.Phys. A377 (1982) 505
15. J. Bystricky, F. Lehar and P. Winternitz, J. Physique (Paris) 39 (1978) 1
16. S.M. Bilenky and R.M. Ryndin, Phys. Lett. 6 (1963) 217
17. R.J.N. Phillips, Nucl. Phys. 43 (1963) 413
18. F. Perrot, H. Azaiez, J. Ball, J. Bystricky, P. Chaumette, Ph. Chesny, J. Derégel, J. Fabre, J.M. Fontaine, J. Gosset, F. Lehar, W.R. Leo, A. de Lesquen, C.R. Newsom, Y. Onel, A. Penzo, L. van Rossum, T. Siemiarczuk, J. Vrzal, C.A. Whitten and J. Yonnet, Nucl. Phys. B278 (1986) 881
19. V.G. Ableev, S. Dzhemukhadze, V.P. Yershov, V.V. Fimushkin, B. Kühn, M.V. Kulikov, A.A. Nomofilov, L. Penchev, Yu.K. Pilipenko, N.M. Piskunov, V.I. Sharov, V.B. Shutov, I.M. Sitnik, E.A. Strokovsky, L.N. Strunov, S.A. Zaporozhets, B. Naumann, L. Naumann and S. Tesch, Nucl. Instrum. Methods A306 (1991) 73
20. V. Ghazikhanian, B. Aas, D. Adams, E. Bleszynski, M. Bleszynski, J. Bystricky, G.J. Igo, T. Jaroszewicz, F. Sperisen, C.A. Whitten, P. Chaumette, J. Derégel, J. Fabre, F. Lehar, A. de Lesquen, L. van Rossum, J. Arvieux, J. Ball, A. Boudard and F. Perrot, Phys. Rev. C43 (1991) 1532
21. J. Bystricky, F. Lehar, A. de Lesquen, A. Penzo, L. van Rossum. J.M. Fontaine, F. Perrot, G. Leleux and A. Nakach: Nucl. Instrum. Methods A234 (1985) 412
22. J. Ball, Ph. Chesny, M. Combet, J.M. Fontaine, R. Kunne, M.C. Lemaire, J.L. Sans, J. Bystricky, C.D. Lac, F. Lehar, A. de Lesquen, M. de Mali, F. Perrot-Kunne, L. van Rossum, P. Bach, Ph. Demierre, G. Gaillard, R. Hess, D. Rapin, Ph. Sormani, J.P. Goudour, R. Binz, A. Klett, E. Rössle, H. Schmitt, L.S. Barabash, Z. Janout, B.A. Khachaturov, Yu. A. Usov, D. Lopiano, H. Spinka, Nucl. Phys. A559 (1993) 477
23. A.N. Prokofiev, V.V. Vikhrov, A.A. Zhdanov, L.S. Azhgirey, N.M. Piskunov, G.D. Stoletov, F. Lehar, Polarimeter for the Deuteron Beam at the JINR Synchrophasotron, Proceedings of the International Seminar "DEUTERON 95", Dubna 1995, to be published
24. J. Ball, Ph. Chesny, M. Combet, J.M. Fontaine, C.D. Lac, J.L. Sans, P. Chaumette, H. Desportes, J. Derégel, G. Durand, J. Fabre, L. van Rossum, D. Hill: Dilution Refrigerator and Solenoid for the FERMILAB Spin Physics Facility, 8th International Symposium on High Energy Spin Physics, Minneapolis, Minnesota, USA, September 12-17, 1988 AIP Conference Proceedings No. 187, N.Y. 1989, Particles and Fields Series 37, Vol. II, 1331 and 1334
25. D.L. Adams, N. Akchurin, N.I. Belikov, J. Bystricky, P. Chaumette, M.D. Corcoran, J.D. Cossairt, J. Cranshaw, J. Derégel, A.A. Derevschikov, G. Durand, H. En'yo, J. Fabre, K. Fukuda, H. Funahashi, Y. Goto, O.A. Grachov, D.P. Grosnick, D.A. Hill, K. Imai, Y. Itow, K. Iwatani, K.W. Krueger, K. Kuroda, M. Laghai, F. Lehar, A. de Lesquen, D. Lopiano, F.C. Luehring, A. Maki, S. Makino, A. Masaike, Yu.A. Matulenko, A.P. Meshanin, A. Michalowicz, D.H. Miller, K. Miyake, T. Nagamine, F. Nessi-Tedaldi, M. Nessi, C. Nguyen, S.B. Nurushev, Y. Ohashi, Y. Onel, D.I. Patalakha, G. Pauletta, A. Penzo, A.L. Read, J.B. Roberts, L. van Rossum, V.L. Rykov, N. Saito, G. Salvato, P. Shiavon, J. Shepard, J. Skeens, V.L. Solovyanov, H. Spinka, R. Takashima, F. Takeutchi, N. Tamura, N. Tanaka, D.G. Underwood, A.N. Vasiliev, A. Villari, J.L. White, S. Yamashita, A. Yokosawa, T. Yoshida and A. Zanetti, Phys. Lett. 261B (1991) 197
26. F. Lehar, B. Adiasevich, V.P. Androsov, N. Angelov, N. Anischenko, V. Antonenko, J. Ball, V.G. Baryshevsky, N.A. Bazhanov, A.A. Belyaev, B. Benda, V. Bodyagin, N. Borisov, Yu. Borzunov, F. Bradamante, E. Bunyatova, V. Burinov, E. Chernykh, M. Combet, A. Datskov, G. Durand, A.P. Dzyubak, J.M. Fontaine, V.A. Get'man, M. Giorgi, L. Golovanov, V. Grebenyuk, D. Grosnick, G. Gurevich, T. Hasegawa, D. Hill, N. Horikawa, G. Igo, Z. Janout, V.A. Kalinnikov, I.M. Karnaukhov, T. Kasprzyk, B.A. Khachaturov, A. Kirillov, Yu. Kisselev, E.S. Kousmine, A. Kovalenko, A.I. Kovaljov, V.P. Ladygin, A. Lazarev, Ph. Leconte, A. de Lesquen, A.A. Lukhanin, S. Mango, A. Martin, V.N. Matafonov, E. Matyushevsky, S. Mironov, A. Neganov, B.S. Neganov, A. Nomofilov, V. Perelygin, Yu. Plis, Yu. Pilipenko, I.L. Pisarev, N. Piskunov, Yu. Polunin, Yu.P. Popkov, A.A. Popov, A.N. Prokofiev, M.P. Rekalo, P. Rukoyatkin, J.L.Sans, M.G. Sapozhnikov, V. Sharov, S. Shilov, Yu. Shishov, I.M. Sitnik, P.V. Sorokin, H. Spinka, E.A. Sporov, L.N. Strunov, A. Svetov, J.J. de Swart, Yu.P. Telegin, I. Tolmashov, S. Trentalange, A. Tsvinev, Yu.A. Usov, V.V. Vikhrov, C. Whitten, S. Zaporozhets, A. Zarubin, A.A. Zhdanov, L. Zolin, Nucl. Instrum. Methods A356 (1995) 58
27. E.I. Bunyatova, R.M. Galimov, S.A. Luchkina, "Investigation of Stable Paramagnetic HMBA Complex in Different Solvents", Preprint JINR 12-82-732, Dubna 1982
28. R. Bernard, P. Chaumette, P. Chesny, J. Derégel, R. Duthil, J. Fabre, C. Lesmond, G. Seite, J. Ball, T.O. Niinikoski, and M. Rieubland, Nucl. Instrum. Methods A249 (1986) 176
29. R. Binz, PhD Thesis: Untersuchung der spinabhängigen Neutron-Proton Wechselwirkung im Energiebereich von 150 bis 1100 MeV, University of Freiburg im Breisgau 1991.
30. R.A. Arndt, I.I. Strakovsky, and R.L. Workman, Phys. Rev. C50 (1994) 2731 (SAID 1995)
31. A.E. Dorokhov, N.I. Kochelev and Yu.A. Zubov, Int. J. Mod. Phys. A8 (1993) 603
32. G.'t Hooft, Phys. Rev. D14 (1976) 3432
33. N.I. Kochelev, 3rd International Symposium "DUBNA DEUTERON-95", Dubna, to be published
34. E.L. Lomon, Colloque de Physique (France) 46 (1985) C2-329

35. P. LaFrance and E.L. Lomon, Phys. Rev. D34 (1986) 1341
36. P. Gonzales, P. LaFrance and E.L. Lomon, Phys. Rev. D35 (1987) 2142
37. E.L. Lomon, 8th International Symposium on High Energy Spin Physics, Minneapolis, Minnesota, USA, September 12–17, 1988 AIP Conference Proceedings No. 187, N.Y. 1989 Particles and Fields Series 37, Vol. I, p.655
38. E.L. Lomon, Colloque de Physique (France) 51 (1990) C6-363
39. C.W. Wong, Prog. in Part. and Nucl.Phys. 8 (1982) 223
40. Yu.S. Kalashnikova, I.M. Narodeckii and Yu.A. Simonov, Yad. Fiz. 46 (1987) 1181, transl. Sov. J. Nucl. Phys. 46 (1987) 689
41. I.P. Auer, E. Colton, W.R. Ditzler, H. Halpern, D. Hill, R.C. Miller, H. Spinka, N. Tamura, J.-J. Tavernier, G. Theodosiou, K. Toshioka, D. Underwood, R. Wagner, and A. Yokosawa, Phys. Rev. Lett. 62 (1989) 2649
42. J. Ball, P.A. Chamouard, M. Combet, J.M. Fontaine, R. Kunne, J.M. Lagniel, J.L. Lemaire, G. Milleret, J.L. Sans, J. Bystricky, F. Lehar, A. de Lesquen, M. de Mali, Ph. Demierre, R. Hess, Z.F. Janout, E.L. Lomon, D. Rapin, B. Vuaridel, L.S. Barabash, Z. Janout, V.A. Kalinnikov, Yu.M. Kazarinov, B.A. Khachaturov, V.N. Matafonov, I.L. Pisarev, A.A. Popov, Yu.A. Usov, M. Beddo, D. Grosnick, T. Kasprzyk, D. Lopiano, H. Spinka, A. Boutefnouchet, V. Ghazikhanian, C.A. Whitten, Phys. Lett. B320 (1994) 206
43. D.V. Bugg, D.C. Salter, G.H. Stafford, R.F. George, K.F. Riley, R.J. Tapper, Phys. Rev. 146 (1966) 980
44. H. Spinka, E. Colton, W.R. Ditzler, H. Halpern, K. Imai, R. Stanek, N. Tamura, G. Theodosiou, K. Toshioka, D. Underwood, R. Wagner, Y. Watanabe, A. Yokosawa, G.R. Burleson, W.B. Cottingame, S.J. Greene, S. Stuart, J.J. Jarmer, Nucl. Instrum. Methods 211 (1983) 239
45. C.D. Lac, J. Ball, J. Bystricky, J. Derégel, F. Lehar, A. de Lesquen, L. van Rossum, J.M. Fontaine, F. Perrot and P. Winternitz, J. Phys. (France) 51 (1990) 2689
46. R. Bertini, J. Arvieux, M. Boivin, J.M. Durand, F. Soga, E. Descroix, J.Y. Grossiord, A. Guichard, J.R. Pizzi, Th. Hennino and L. Antonuk, Phys. Lett. 162B (1985) 77
47. R. Bertini, G. Roy, J.M. Durand, J. Arvieux, M. Boivin, A. Boudard, C. Kerboul, J. Yonnet, M. Bedjidian, J.Y. Grossiord, A. Guichard, J.R. Pizzi, Th. Hennino and L. Antonuk, Phys. Lett. 203B (1988) 18
48. J. Yonnet, R. Abegg, M. Boivin, A. Boudard, G. Bruge, P. Couvert, G. Gaillard, M. Garçon, L.G. Greeniaus, D.A. Hutcheon, C. Kerboul and B. Mayer, Nucl. Phys. A562 (1993) 352
49. P. LaFrance and E.L. Lomon, Proceedings of International Conference on "Mesons and Nuclei at Intermediate Energies", Dubna, 3-7 Mai 1994, Editors M.Kh. Khankhasayev and Zh.B. Kurmanov, World Scientific, Singapore 1995-XV, p.97
50. J. Bystricky, C. Lechanoine-Leluc and F. Lehar, J. Physique (France) 51 (1990) 2747
51. J. Bystricky, C. Lechanoine-Leluc, F. Lehar, J. Physique (Paris) 48 (1987) 199

Eur. Phys. J. C 13, 255–265 (2000)
Digital Object Identifier (DOI) 10.1007/s100520000321

THE EUROPEAN PHYSICAL JOURNAL C

Measurements of the np total cross section difference $\Delta\sigma_L$ at 1.59, 1.79 and 2.20 GeV

V.I.Sharov[1], S.A.Zaporozhets[1], B.P.Adiasevich[2], N.G.Anischenko[1], V.G.Antonenko[2], L.S.Azhgirey[3], V.D.Bartenev[1], N.A.Bazhanov[4], N.A.Blinov[1], N.S.Borisov[3], S.B.Borzakov[5], Yu.T.Borzunov[1], L.V.Budkin[3,†], V.F.Burinov[3], Yu.P.Bushuev[1], L.P.Chernenko[5], E.V.Chernykh[1], S.A. Dolgii[1], V.M.Drobin[1], G.Durand[6], A.P.Dzyubak[7], A.N.Fedorov[8], V.V.Fimushkin[1], M.Finger[3,9], M.Finger,Jr.[3], L.B.Golovanov[1], G.M.Gurevich[10], A.Janata[3,11], A.V.Karpunin[1,†], B.A.Khachaturov[3], A.D.Kirillov[1], A.D.Kovalenko[1], A.I.Kovalev[4], V.G.Kolomiets[3], A.A.Kochetkov[12], E.S.Kuzmin[3], V.P.Ladygin[1], A.B.Lazarev[3], F.Lehar[6], A. de Lesquen[6], A.A.Lukhanin[7], P.K.Maniakov[1], V.N.Matafonov[3], A.B.Neganov[3], M.S.Nikitina[12], G.P.Nikolaevsky[1], A.A.Nomofilov[1], Tz.Panteleev[5,13], Yu.K.Pilipenko[1], I.L.Pisarev[3], N.M.Piskunov[1], Yu.A.Plis[3], Yu.P.Polunin[2], A.N.Prokofiev[4], P.A.Rukoyatkin[1], O.N.Shchevelev[3], V.A.Shchedrov[4], S.N.Shilov[3], Yu.A.Shishov[1], V.B.Shutov[1], M.Slunečka[3,9], V.Slunečková[3], A.Yu.Starikov[1], G.D.Stoletov[3], L.N.Strunov[1], A.L.Svetov[1], A.P.Tsvinev[1], Yu.A.Usov[3], V.I.Volkov[1], V.P.Yershov[1], A.A.Zhdanov[4], V.N.Zhmyrov[3]

[1] Laboratory of High Energies, JINR, 141980 Dubna, Moscow region, Russia
[2] Russian Scientific Center "Kurchatov Institute", Kurchatova Street 46, 123182 Moscow, Russia
[3] Laboratory of Nuclear Problems, JINR, 141980 Dubna, Moscow region, Russia
[4] Petersburg Nuclear Physics Institute, High Energy Physics Division, 188350 Gatchina, Russia
[5] Frank Laboratory of Neutron Physics, JINR, 141980 Dubna, Moscow region, Russia
[6] DAPNIA, CEA/Saclay, 91191 Gif-sur-Yvette Cedex, France
[7] Kharkov Institute of Physics and Technology, Akademicheskaya Street 1, 310108 Kharkov, Ukraine
[8] Laboratory of Particle Physics, JINR, 141980 Dubna, Moscow region, Russia
[9] Charles University, Faculty of Mathematics and Physics, V Holešovičkách 2, 18000 Praha 8, Czech Republic
[10] Russian Academy of Sciences, Institute for Nuclear Research, 60th Oct. Aniversary Prospect 7A, 117312 Moscow, Russia
[11] Academy of Sciences of the Czech Republic, Nuclear Research Institute, 25068 Řež, Czech Republic
[12] Moscow State University, Faculty of Physics, 119899 Moscow, Russia
[13] Bulgarian Academy of Sciences, Institute for Nuclear Research and Nuclear Energy, Tsarigradsko shaussee boulevard 72, 1784 Sofia, Bulgaria

Received: 19 August 1999 / Published online: 3 February 2000 – © Springer-Verlag 2000

This paper is dedicated to the memory of Rostislav Mikhailovich Ryndin, one of the principal founders of relations for the nucleon-nucleon spin-dependent total cross sections.

Abstract. New results of the neutron-proton spin-dependent total cross section difference $\Delta\sigma_L(np)$ at the neutron beam kinetic energies 1.59, 1.79 and 2.20 GeV are presented. Measurements were performed at the Synchrophasotron of the Laboratory of High Energies of the Joint Institute for Nuclear Research in Dubna. A quasi-monochromatic neutron beam was produced by break-up of extracted polarized deuterons. Neutrons were transmitted through a large polarized proton target. Measurements were performed either with a parallel or an antiparallel beam and target polarizations, both oriented along the beam momentum. The results at the two higher energies were measured with two opposite beam and target polarization directions. Only one target polarization direction was available at 1.59 GeV. The present measurements agree well with existing data. A fast decrease of the $-\Delta\sigma_L(np)$ values with increasing energy above 1.1 GeV was confirmed. The new results are also compared with model predictions and with phase shift analysis fits. The $\Delta\sigma_L$ quantities for isosinglet state I=0, deduced from the measured $\Delta\sigma_L(np)$ values and known $\Delta\sigma_L(pp)$ data, are given.

† Deseased

1 Introduction

In this paper are presented the new results of the spin-dependent neutron-proton total cross section difference $\Delta\sigma_L(np)$, measured in 1997 with a quasi-monochromatic polarized neutron beam and a polarized proton target (PPT). Results were obtained at the central values of 1.59, 1.79 and 2.20 GeV neutron beam kinetic energies.

The free polarized neutron beam was produced by break-up of polarized deuterons accelerated by the Synchrophasotron of the Laboratory of High Energies (LHE) of the Joint Institute for Nuclear Research (JINR) in Dubna. This accelerator provides the highest energy polarized neutron beam, which can be reached now (3.7 GeV).

The measurements were carried out within the nucleon-nucleon experimental program which started in 1995 [1,2]. The aim of the program is to extend studies of np interactions above 1.1 GeV.

For purposes of $\Delta\sigma_L(np)$ measurements, a large Argonne-Saclay polarized proton target (PPT) was reconstructed at Dubna [3,4] and a new polarized neutron beam line [5,6] was used. A set of dedicated neutron detectors with corresponding electronics and data acquisition system [7] were performed. At the beginning of 1995, the first three $\Delta\sigma_L(np)$ data points were successfully measured at the central energies 1.19, 2.49, and 3.65 GeV [1,2]. For purposes of the measurements in 1997, a new PPT polarizing solenoid [8] was developed in LHE.

The nucleon-nucleon (NN) total cross section differences $\Delta\sigma_L$ and $\Delta\sigma_T$ together with the spin-average total cross section σ_{0tot} are measured in pure inclusive transmission experiments. They are linearly related with three non-vanishing imaginary parts of the NN forward scattering amplitudes via optical theorems. They check predictions of available dynamic models and provide an important contribution to databases of phase-shift analyses (PSA). From the measured data it is possible to deduce the $\Delta\sigma_L$ nucleon-nucleon isosinglet ($I = 0$) parts using the existing pp (isotriplet $I = 1$) results.

The total cross section differences for pp scattering were first measured at the ANL-ZGS (USA) and then at TRIUMF (Canada), PSI (Switzerland), LAMPF (USA) and SATURNE II (France). Results cover the energy range from 0.2 to 12 GeV. Other data were measured at 200 GeV at FERMILAB (USA) for pp and $\bar{p}p$ interactions [9]. Measurements with incident charged particles need a different experimental set-up than neutron-proton experiments due to the contribution of electromagnetic interactions. Existing results are discussed in review [10] and in references therein.

For the first time $\Delta\sigma_L(pn)$ results from 0.51 to 5.1 GeV were deduced in 1981 from the $\Delta\sigma_L(pd)$ and $\Delta\sigma_L(pp)$ measurement at the ANL-ZGS [11]. Taking a simple difference between pd and pp results, corrected only for Coulomb-nuclear rescattering and deuteron break-up, yields data in qualitative agreement with the free np results. Correction for Glauber-type rescattering including 3-body state final interactions [12] provides a disagreement [10]. For these reasons, the ANL-ZGS pn results were omitted in many existing PSA databases.

Using free polarized neutrons at SATURNE II, $\Delta\sigma_T$ and $\Delta\sigma_L$ results were obtained at 11 and 10 energies, respectively in the energy range 0.31 and 1.10 GeV [13,14,15]. The Saclay results were soon followed by PSI measurements [16] at 7 energy bins from 0.180 to 0.537 GeV, using a continuous neutron energy spectrum. The PSI and Saclay sets allowed to deduce imaginary parts of np and $I = 0$ spin-dependent forward scattering amplitudes [10,15].

$\Delta\sigma_L(np)$ has also been measured at five energies between 0.484 and 0.788 GeV at LAMPF [17]. A quasi-monoenergetic polarized neutron beam was produced in $pd \Rightarrow n + X$ scattering of longitudinally polarized protons. Large neutron counter hodoscopes have to be used because of the small neutron beam intensity.

To be complete, at low energies, $\Delta\sigma_L(np)$ at 66 MeV was measured at the PSI injector [18], and at 16.2 MeV in Prague (Czech Republic) [19]. $\Delta\sigma_T(np)$ was determined in TUNL (USA) at 9 energies between 3.65 and 11.6 MeV [20], and at 16.2 MeV in Prague [21]. Recently, in TUNL $\Delta\sigma_L(np)$ was measured at 6 energies between 4.98 and 19.7 MeV [22] and $\Delta\sigma_T(np)$ at 3 other energies between 10.7 and 17.1 MeV [23]. The results [22,23] are still unpublished, but appear in the George Washington University and Virginia Polytechnic Institute (GW/VPI) PSA database [24] (SAID SP99).

Only $\Delta\sigma_L(np)$ results were obtained at the JINR accelerator at high energy. All these results smoothly connect with the existing data at lower energies. The $-\Delta\sigma_L(np)$ energy dependence show a fast decrease to zero between 1.1 and 2.0 GeV. The data are compared with model predictions and with the PSA fits. Values of the $I = 0$ part of $\Delta\sigma_L$ are also presented.

In Sect. 2 we give a brief determination of observables. In Sect. 3 is described the method of the measurement and an incomplete target filling is treated. The essential details concerning the beam, the polarimeters, the experimental set-up and PPT are given in Sect. 4. The data acquisition and analyses are described in Sect. 5. The results and discussion are presented in Sect. 6.

2 Determination of observables

Throughout this paper we use the NN formalism and the notations for the elastic nucleon-nucleon scattering observables from [25].

The general expression of the total cross section for a polarized nucleon beam transmitted through a PPT, with arbitrary directions of beam and target polarizations, $\vec{P}_B$ and $\vec{P}_T$, respectively, was first deduced in [26,27]. Taking into account fundamental conservation laws, it is written in the form :

$$\sigma_{tot} = \sigma_{0tot} + \sigma_{1tot}(\vec{P}_B, \vec{P}_T) + \sigma_{2tot}(\vec{P}_B, \vec{k})(\vec{P}_T, \vec{k}), \quad (2.1)$$

where $\vec{k}$ is a unit vector in the direction of the beam momentum. The term σ_{0tot} is the total cross section for unpolarized particles, σ_{1tot}, σ_{2tot} are the spin-dependent contributions. They are related to the measurable observables

$\Delta\sigma_T$ and $\Delta\sigma_L$ by :

$$-\Delta\sigma_T = 2\sigma_{1tot}, \tag{2.2}$$

$$-\Delta\sigma_L = 2(\sigma_{1tot} + \sigma_{2tot}), \tag{2.3}$$

called "total cross section differences". The negative signs for $\Delta\sigma_T$ and $\Delta\sigma_L$ in (2.2) and (2.3) correspond to the usual, although unjustified, convention in the literature. The total cross section differences are measured with either parallel or antiparallel beam and target polarization directions. Polarization vectors are transversally oriented with respect to $\vec{k}$ for $\Delta\sigma_T$ measurements and longitudinaly oriented for $\Delta\sigma_L$ experiments. Only $\Delta\sigma_L$ measurements are treated below, but the formulae are similar for both total cross section differences.

For $\vec{P}_B^{\pm}$ and $\vec{P}_T^{\pm}$, all oriented along $\vec{k}$, we obtain four total cross sections :

$$\sigma(\rightrightarrows) = \sigma(++) = \sigma_{0tot} + |P_B^+ P_T^+|\ (\sigma_{1tot} + \sigma_{2tot}), \tag{2.4a}$$

$$\sigma(\leftrightarrows) = \sigma(-+) = \sigma_{0tot} - |P_B^- P_T^+|\ (\sigma_{1tot} + \sigma_{2tot}), \tag{2.4b}$$

$$\sigma(\rightleftarrows) = \sigma(+-) = \sigma_{0tot} - |P_B^+ P_T^-|\ (\sigma_{1tot} + \sigma_{2tot}), \tag{2.4c}$$

$$\sigma(\leftleftarrows) = \sigma(--) = \sigma_{0tot} + |P_B^- P_T^-|\ (\sigma_{1tot} + \sigma_{2tot}). \tag{2.4d}$$

The signs in brackets correspond to the $\vec{P}_B$ and $\vec{P}_T$ directions with respect to $\vec{k}$, in this order. In principle, an arbitrary pair of one parallel and one antiparallel beam and target polarization directions determines $\Delta\sigma_L$. By using two independent pairs, we also remove an instrumental asymmetry.

In the following, we will consider the neutron beam and the proton target. Since the $\vec{P}_B$ direction at the Synchrophasotron could be reversed every cycle of the accelerator, it is preferable to calculate $\Delta\sigma_L$ from pairs of ($\rightrightarrows$ and ($\leftrightarrows$), or ($\rightleftarrows$) and ($\leftleftarrows$) measurements with the same $\vec{P}_T$ orientation to avoid long-time efficiency fluctuations of the neutron detectors. Values of $|P_T^+|$ and $|P_T^-|$ are considered to be well known as functions of time. The spin-independent term drops out when taking the difference, and one obtains :

$$\begin{aligned} -\Delta\sigma_L(P_T^+) &= 2\ (\sigma_{1tot} + \sigma_{2tot})^+ \\ &= \frac{2\ [\sigma(\rightrightarrows) - \sigma(\leftrightarrows)]}{(|P_B^+| + |P_B^-|)\ |P_T^+|}, \end{aligned} \tag{2.5a}$$

$$\begin{aligned} -\Delta\sigma_L(P_T^-) &= 2(\sigma_{1tot} + \sigma_{2tot})^- \\ &= \frac{2\ [\sigma(\leftleftarrows) - \sigma(\rightleftarrows)]}{(|P_B^+| + |P_B^-|)\ |P_T^-|}, \end{aligned} \tag{2.5b}$$

The asymmetry, proportional to the mean value of

$$|P_B| = \frac{1}{2}(|P_B^+| + |P_B^-|), \tag{2.6}$$

is continuously monitored by a beam polarimeter.

The instrumental asymmetry cancels out, giving the final results as a simple average

$$\Delta\sigma_L = \frac{1}{2}[\Delta\sigma_L(P_T^+) + \Delta\sigma_L(P_T^-)]. \tag{2.7}$$

This is discussed in detail in Sect. 4.

σ_{0tot}, $\Delta\sigma_T$ and $\Delta\sigma_L$ are linearly related to the imaginary parts of the three independent forward scattering invariant amplitudes $a + b$, c and d via optical theorems:

$$\sigma_{0tot} = (2\pi/K)\ \Im m\ [a(0) + b(0)], \tag{2.8}$$

$$-\Delta\sigma_T = (4\pi/K)\ \Im m\ [c(0) + d(0)], \tag{2.9}$$

$$-\Delta\sigma_L = (4\pi/K)\ \Im m\ [c(0) - d(0)], \tag{2.10}$$

where K is the CM momentum of the incident nucleon. The relations (2.9) and (2.10) allow to extract the imaginary parts of the spin-dependent invariant amplitudes $c(0)$ and $d(0)$ at the angle $\theta = 0°$ from the measured values $\Delta\sigma_L$ and $\Delta\sigma_T$. Note that the optical theorems provide the absolute amplitudes. Using a direct reconstruction of the scattering matrix (DRSA) these absolute amplitudes are determined at $\theta = 0°$ only, whereas at any other angle one common phase remains undetermined. The absolute amplitudes are also determined by PSA at any scattering angle. The PSA and DRSA approaches are complementary phenomenological analyses, as discussed in [28,29].

Using the measured $\Delta\sigma(np)$ values and the existing $\Delta\sigma(pp)$ data at the same energy, one can deduce $\Delta\sigma_{L,T}(I = 0)$ as :

$$\Delta\sigma_{L,T}(I = 0) = 2\Delta\sigma_{L,T}(np) - \Delta\sigma_{L,T}(pp). \tag{2.11}$$

3 Method of measurement

In the transmission experiment we measure which part of incident beam particles remains in the beam after transmission. For the experiments with incident neutrons such a measurement is always relative. The neutron beam has a circular profile, given by preceeding beam collimators. Out of the collimator dimension the neutron flux is zero, within the collimator size the flux is uniform. The neutron beam intensity is monitored by neutron beam monitors, placed upstream from the target. The target material consists of small beads placed in a cylindrical container of the circular profile. The container cover the beam spot and its horizontal axis coincide with the beam axis. The transmission detectors, downstream from the target, are larger than the beam dimensions. Any unscattered beam particle is detected with the same probability.

If N_{in} is the number of neutrons entering the target and N_{out} the number of neutrons transmitted in a counter array of solid angle Ω, then the total cross section $\sigma(\Omega)$ is related to measured quantities :

$$\frac{N_{out}}{N_{in}} = \exp\big(-\sigma(\Omega) \times n \times d\big) = \exp(-F), \tag{3.1}$$

where n is the number of all target atoms per cm^3 d is the target length and N_{out}/N_{in} is the simple transmission ratio. The number of counts of the beam monitor M and of the transmission counter T depend on the efficiency of each detector, i.e. $M = N_{in} \times \eta(M)$ and $T = N_{out} \times \eta(T)$. The extrapolation of $\sigma(\Omega)$ towards $\Omega = 0$ gives the unpolarized total cross section σ_{0tot}.

In the case of an incompletely filled target, the beads inside the container may be differently distributed. Two hypothetical configurations of the beads represent limits to be considered. The first limit occurs, if a lower part of the container cylinder is full over the entire length of the target d and the upper part is empty. Let us call this filling mode "horizontal" (H). The second limit occurs, if the same amount of the material in the container is condensed within a smaller length and cover the beam spot. This kind of filling will be called "vertical" (V). The transmission effect of any other possible bead configuration will be in between the effects of these two filling modes, since an arbitrary bead distribution could be approximated by a flight of stairs. Decreasing the steps of stairs, we obtain any possible shape of the bead volume.

Introducing a filling factor a ($0 \leq a \leq 1$) the transmission ratio for the horizontal and vertical filling modes can be written as

$$NH_{out}/N_{in} = \big(a\ \exp(-F)\big) + (1-a) \qquad (3.2a)$$
$$NV_{out}/N_{in} = \exp(-F\ a)\ . \qquad (3.2b)$$

In the $\Delta\sigma_L(\Omega)$ measurements with a full target, only the number of polarizable hydrogen atoms n_H is important. $\sigma_{tot}(\Omega)$ depends on the polarizations $P_B^{\pm}$ and $P_T^{\pm}$ as shown in (2.4). For $\Omega \to 0$, we obtain $\Delta\sigma_L(\Omega) \to \Delta\sigma_L$. If one sums over the events taken with one fixed target polarizations P_T^+ or P_T^- and using (2.5a) or (2.5b), the double transmission ratios of the measurements with the averaged P_B from (2.6) for the two $\vec{P}_T$ directions become :

$$\frac{N_{out}(++)/N_{in}(++)}{N_{out}(-+)/N_{in}(-+)} = \exp\ (-\Delta\sigma_L(\Omega)\ |P_B\ P_T^+|\ n_H\ d) \qquad (3.3a)$$
$$\frac{N_{out}(--)/N_{in}(--)}{N_{out}(+-)/N_{in}(+-)} = \exp\ (-\Delta\sigma(\Omega)\ |P_B\ P_T^-|\ n_H\ d)\ . \qquad (3.3b)$$

Note that we follow the notation of (2.3).

Thus the neutron detector efficiencies drop out. In the following we put $N = N_{out}/N_{in}$ depending of $\vec{P}_B$ and $\vec{P}_T$ combination and (3.3) provide :

$$-\Delta\sigma_L(\Omega, P_T^+) = \frac{1}{|P_B\ P_T^+|\ n_H\ d} \times \ln\ \left(\frac{N(++)}{N(-+)}\right), \qquad (3.4a)$$
$$-\Delta\sigma_L(\Omega, P_T^-) = \frac{1}{|P_B\ P_T^-|\ n_H\ d} \times \ln\ \left(\frac{N(--)}{N(+-)}\right). \qquad (3.4b)$$

We may neglect the extrapolation of $\Delta\sigma_L(\Omega)$ towards $\Omega = 0$ due to the small sizes of detectors [1,2]. The Saclay-Geneva (SG) PSA [29] at 1.1 GeV shows that for the angles covered by our detectors the resulting $-\Delta\sigma_L$ value decreases by 0.04 mb at this energy. The SG-PSA solution at 1.0 GeV suggests that this possible error decreases with increasing energy.

The ratio of n_H to other target nuclei depends on the target material. The presence of carbon in the PPT beads add the term $\sigma_{tot}(C)$ in (2.4). This term is spin-independent and its contribution drops out in differences (2.5). The same occurs for ^{16}O and ^4He in the target and for the cryogenic envelopes. The np total cross section for all unpolarized atoms is large with respect to the total cross section difference. Above ~ 0.3 GeV neutron beam kinetic energy any existing polarized target may be always considered to be very thin for $\Delta\sigma_L(np)$ experiment and we can replace the exponential functions in (3.3) by linear ones. We obtain :

$$-\Delta\sigma_L(P_T^+) = \frac{1}{|P_B\ P_T^+|\ n_H\ d} \times \left(1 - \frac{N(++)}{N(-+)}\right), \qquad (3.5a)$$
$$-\Delta\sigma_L(P_T^-) = \frac{1}{|P_B\ P_T^-|\ n_H\ d} \times \left(1 - \frac{N(--)}{N_(+-)}\right). \qquad (3.5b)$$

At any JINR accelerator energy this approximation provides an error smaller that 6×10^{-7} and can never be recognized.

However, there are small contributions from ^{13}C and ^3He, which may be slightly polarized. This contribution was estimated to be $\pm$ 0.3 % in [1,2].

For $\Delta\sigma_L$, without a lost of generality, we will consider only one $|P_T| = P_T^+$ sign and we denote the effect, measured with a completely filled target in ((3.3a) as

$$\exp(-E) = \exp(-\frac{1}{2}\Delta\sigma_L\ |P_B\ P_T|\ n_H\ d\ ). \qquad (3.6)$$

Using (2.4a), (2.4b) and the horizontal mode of the incomplete target filling, we obtain

$$\frac{NH(++)}{NH(-+)} = \frac{a \times \exp\ (-F) \times \exp\ (-E) + (1-a)}{a \times \exp\ (-F) \times \exp(+E) + (1-a)}. \qquad (3.7)$$

Below we will considered F from (3.1) as the unpolarized background from all target atoms. We put $\exp(\pm\ E) = 1 \pm\ E$, and rewrite (3.7) :

$$\frac{NH(++)}{NH(-+)} = \frac{1 - \dfrac{E\ a\ \exp(-F)}{a\ \exp(-F) + (1-a)}}{1 + \dfrac{E\ a\ \exp(-F)}{a\ \exp(-F) + (1-a)}} \qquad (3.8)$$

We applied the binomial development $(1-x)/(1+x) \simeq (1-2x)$ for small x. In our case the error is smaller than 2×10^{-6}. Using this, we obtain the relation for $-\Delta\sigma_L$, similar to (3.5) :

$$-\Delta\sigma_L = \frac{1}{|P_B\ P_T|\ n_H\ d\ C_{corr}} \times \left(1 - \frac{NH(++)}{NH(-+)}\right). \qquad (3.9)$$

The multiplicative correction factor

$$C_{corr} = \frac{a\ \exp(-F)}{a\ \exp(-F) + (1-a)}, \qquad (3.10)$$

depends on a and on the background, but is independent on the measured $\Delta\sigma_L$ value. It holds $C_{corr} \leq a$ where the equality is valid for $\exp(-F) = 1$, i.e no background. The equality also occurs, if the same amount of the target material is condensed in a shorter target (vertical filling mode) of the length $d \times a$.

4 Experimental set-up

The $\Delta\sigma_L(np)$ experimental set-up was described in [1,2]. We mention here only essential items, which are important for the data analysis and results, as well as modifications and improvements of the apparatus and of the experimental conditions.

Figure 1 shows both polarized deuteron and polarized free neutron beam lines [5,6], the two polarimeters [30,31], the neutron production target (BT), the collimators, the spin rotation magnet (SRM), PPT [3,4,32], the neutron monitors M1, M2, transmission detectors T1, T2, T3 and the neutron beam profile monitor NP. The associated electronics was described in [1,2] and the data acquisition system in [7].

Accelerated deuterons were extracted at energies 3.20, 3.60 and 4.40 GeV for the $\Delta\sigma_L(np)$ measurements as well as at 1.60 GeV for the polarimetry purposes. Their beam momenta p_d were known with the relative accuracy of $\sim \pm 1$ %. The intensity of primary polarized deuteron beam was increased by a factor $\sim$ 3 to 4 with respect to the 1995 run. The average deuteron intensity over the run was $2.12\times10^9 d$/cycle. It was continuously monitored using two calibrated ionization chambers placed in the focal points F3 and F4 of the deuteron beam line.

The beam of free quasi-monochromatic neutrons, polarized along the vertical direction, was obtained by break-up at 0° of vector polarized deuterons in BT. Neglecting the BT thickness, neutrons have a laboratory momentum $p_n = p_d/2$ with a momentum spread of FWHM $\simeq$ 5 % [33]. BT contained 20 cm Be with the cross section of 8×8 cm^2. The passage of deuterons through air, windows and the BT matter provided a decrease of the deuteron beam energy by 20 MeV in the BT center and the mean neutron energy decreased by 10 MeV [1,2]. For the results the energies and laboratory momenta in the BT center are quoted, for the beam polarization measurements the extracted beam energies were used.

The values and directions of the neutron and proton beam polarizations after break-up, $\vec{P}_B(n)$ and $\vec{P}_B(p)$, respectively, are the same as the vector polarization $\vec{P}_B(d)$ of the incident deuteron beam [34,35].

The measurement of $P_B(d)$ was carried out by the four-arm *dp* beam line polarimeter [30]. Deuterons, scattered on the liquid hydrogen target, were analyzed by a magnetic field. The *dp* polarimeter may use a high intensity of deuterons. It accurately determined the elastic *pd* scattering asymmetry at $T_{kin}(d) = 1.60$ GeV, where the analyzing power of this reaction is well known, and at the four-momentum transfer square t = –0.015 (GeV/c)^2 ($\theta_{lab}(d) \sim 7.7°$), close to the maximal analyzing power value [36]. In principle, the $P_B(d)$ needs to be determined at one energy only, since no depolarizing resonance exists [30]. On the other hand, the measurement requires to change the deuteron energy and to extract deuterons in another beam line, which is a time-consuming operation. This polarimeter was used only once before the data acquisition and gives an average for positive and negative signs of the vector polarization $|P_B(d)| = 0.524 \pm 0.010$. A possible absolute systematic error of this measurement is $\pm$0.010.

Another four-arm beam polarimeter [31] with small acceptance of 7.1×10^{-4} sr continuously monitored $P_B(p)$ value during the data acquisition. The deuteron beam, considered as a beam of quasifree protons and neutrons, was scattered on CH_2 target at 14° lab. This polarimeter measured the *pp* left-right asymmetry on hydrogen and carbon at $T_{kin}(p) = T_{kin}(d)/2$. At $T_{kin}(p) = 0.800$ GeV, the simultaneous measurement together with the *dp* polarimeter gave the asymmetry $\epsilon(CH_2) = 0.2572 \pm 0.0071$. A subtraction of the carbon and inelastic contributions provided the *pp* asymmetry on hydrogen $\epsilon(pp) = 0.2661 \pm 0.0073$.

The *pp* analyzing power A_{oono} was taken from the energy fixed GW/VPI-PSA [24] (SP99, solution 0.800 GeV) as well as from SG-PSA [29] (solution 0.795 GeV). The $A_{oono}(pp)$ predictions at 0.800 GeV were:

GW/VPI-PSA ... 0.4871 ± 0.0034,
SG-PSA ... 0.4821 ± 0.0009.

The mean value $A_{oono}(pp) = 0.4846 \pm 0.0017$ and the measured asymmetry provided $P_B(p)| = |P_B(d)| = 0.549 \pm 0.015$.

The weighted average of both independent results from the two polarimeters gives

$$|P_B(p)| = 0.532 \pm 0.008,$$

used for the calculations of the present $\Delta\sigma_L$ data. This is in excellent agreement with the value $|P_B(n)| = |P_B(d)| = 0.533 \pm 0.009$ measured in 1995 with the *dp* polarimeter at $T_{kin}(d) = 1.662$ GeV and used in [1,2].

Also in 1995, at 0.831 GeV, the *pp* polarimeter provided $\epsilon(CH_2) = 0.246 \pm 0.016$ only. If we apply the present ratio of $\epsilon(pp)/\epsilon(CH_2) = 1.0346$, neglecting the small energy difference, we have $\epsilon(pp) = 0.255 \pm 0.017$. The discrete energy $A_{oono}(pp)$ predictions from GW/VPI-PSA [24] (SP99, solution 0.850 GeV) and from SG-PSA [29] (solution 0.834 GeV) give the mean value of 0.4824 ± 0.0048. We obtain $P_B(p)| = |P_B(d)| = 0.528 \pm 0.035$, in agreement with the former *dp* polarimeter value.

Note that we have used the discrete energy PSA for the *pp* analyzing power calculations. Both PSA are locally energy dependent and describe the measured observables at its own energies. The energy dependent PSA is not an adequate tool for the polarimetry purposes, since the A_{oono} fit at a given energy may be smeered by all other observables fitted in a wide energy range.

We observed that $|P_b(d)|$ decreased during the running time *tm* (hours) as

$$P_d(tm) = P_d(tm = 0)\ (1 - 0.00154 \cdot tm)\ . \qquad (4.1)$$

The error of the linear term is $\pm$ 0.00013. This decrease, due to an unknown effect in the ion source was independent on the beam energy and was taken into account for the present results. The global relative systematic error of $|P_b(d)|$ from all sources was $\pm$1.7 %.

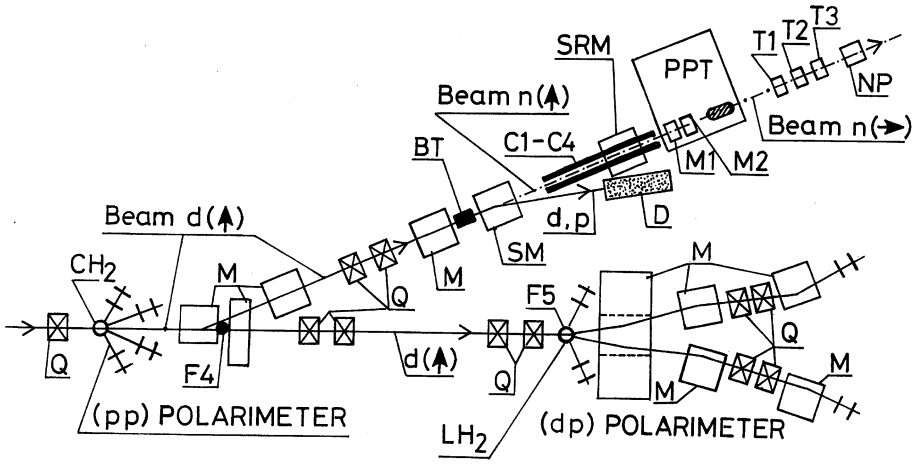

Fig. 1. Layout of the beam lines in the experimental hall (not in the scale). The meaning of the symbols: full lines ... vector polarized deuteron beams with $\vec{P}_B(d)$ oriented along the vertical direction $d(\uparrow)$, dash-dotted line ... polarized neutron beam, $n(\uparrow)$ ... neutrons polarized vertically, $n(\rightarrow)$ ... neutrons polarized longitudinally, BT ... neutron production target, D ... beam-dump for charged particles, SM ... sweeping magnet, SRM ... spin rotating magnet M ... dipole magnets, Q ... quadrupoles, C1 to C4 ... neutron beam collimators, M1, M2, T1, T2, T3, neutron detectors, PPT ... polarized proton target, NP ... neutron beam profile monitor, LH_2 ... liquid hydrogen target of the *dp* polarimeter, CH_2 ... target of the *pp* polarimeter, F4, F5 ... focal points

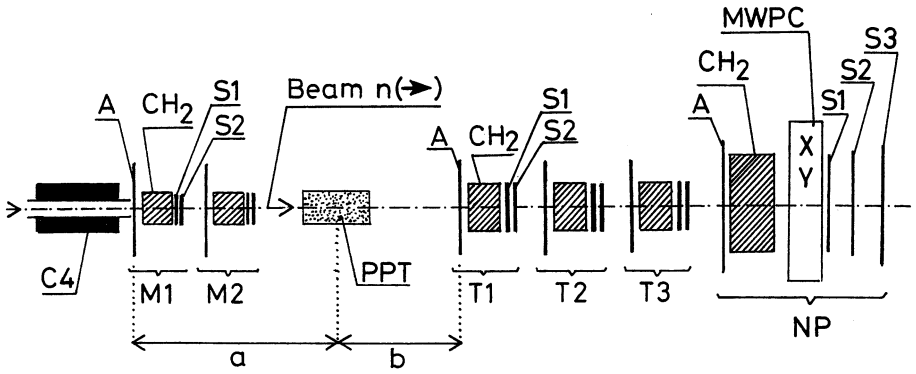

Fig. 2. Experimental set-up for the $\Delta\sigma_L(np)$ measurement (not in the scale). The meaning of the symbols: C4 ... last neutron beam collimator, 25 mm in diameter, M1, M2 ... monitor neutron detectors, T1, T2, T3 ... transmission neutron detectors, NP ... neutron beam profile monitor, CH_2 ... radiators (dimensions in text), A ... anticoincidence scintillation counters, S1, S2, S3 concidence scintillation counters, MWPC ... two multi-wire proportional chambers, distance a = 235 cm, distance b = 655 cm

The dimensions and positions of the iron and brass collimators C1-C4 (Fig. 1) were as described in [1,2]. The accurate measurement of the collimated neutron beam profiles were performed in a dedicated run, using nuclear emulsions. During the data acquisition, the position and the X,Y-profiles of the neutron beam were continuously monitored by the neutron beam profile monitor (NP), placed close downstream from the last transmission detector.

In order to rotate the neutron beam polarization from the vertical to the longitudinal direction, a spin-rotating magnet (SRM) was used. The SRM field map was carefully measured and the magnetic field was continuously monitored by a Hall probe. The uncertainty of the magnetic field integral within the neutron beam path area may provide a small additional systematic error of ± 0.2 %.

The frozen-spin polarized proton target, reconstructed to the movable device [3,4,8,32] was used. The target material was 1,2-propanediol ($C_3H_8O_2$) with a paramagnetic Cr^V impurity having the spin concentration of 1.5×10^{20} cm^{-3} [37]. The propanediol beads were loaded in a thin-wall teflon container 200 mm long and 30 mm in diameter, placed inside the dilution refrigerator.

The weight of the propanediol beads for the completely filled container is W = 94.88 g and the total number of polarizable hydrogen atoms on the beam neutron path gives $n_H \times d = 8.878\ 10^{23}$ cm^{-2}. In the present experiment the measured weight of the beads was W' = (73.25 $+0.80, -0.20$) g. The ratio of the weights is a = W'/W = 0.772. For our $\Delta\sigma_L$ calculation we have considered the horizontal filling mode of (3.9). The correction factor C_{corr} is a function of a and weakly depends on the background, as defined in (3.10). The background transmission ratio for the completely filled target was measured in [1,2] and gave $\exp(-F) = 0.779$. Using those values we obtain $C_{corr} = 0.725$ and $n_H\ d\ C_{corr} = (6.44 \pm 0.19)\ 10^{23}$ cm^{-2}. Since in our energy region the spin-averaged total cross sections are fairly constant, we have neglected a possible dependence of C_{corr} on energy. The relative systematic error of ± 1.5 % covers this uncertainty and was included in the final error in quadrature. The $\Delta\sigma_L$ results were calculated using (3.9) with the transmission ratios measured separately for P_T^+ and P_T^-.

We note that for a shorter target of the beam diameter size $C_{corr} = a$ and $n_H \times d \times a = 6.854\ 10^{23}$ cm^2. The difference of these two filling modes is 6.4 %.

The P_T measurements were carried out using a computer-controlled NMR system. The values of negative proton polarization were –0.772 at the beginning of data taking and –0.701 at the end (after 64 hours). The positive

Table 1. Total statistics of recorded events after the first step of the data analysis as functions of energy and the P_B and P_T signs. The count numbers for the monitors M1, M2 and the transmission detectors T1, T2 and T3 are given in 10^6 units. Here 2 ΣT/3 ΣM is calculated from the global statistics of the three transmission detectors and of the two monitors. The energy of neutrons produced in the BT center is given

T_{kin}	Sign		Statistics of detectors					$2\Sigma T/3\Sigma M$
(GeV)	P_B	P_T	M1	M2	T1	T2	T3	
1.59	+	+	4.9985	4.9483	4.3994	4.2241	3.9690	0.84399
1.59	−	+	5.0030	4.9460	4.4048	4.2299	3.9715	0.84472
1.79	+	+	7.8152	7.6557	6.7115	6.4426	6.0965	0.83213
1.79	−	+	7.8170	7.6798	6.7151	6.4392	6.0976	0.82928
1.79	+	−	12.2593	12.0137	10.3517	10.0732	9.4718	0.82112
1.79	−	−	12.2687	12.0306	10.3570	10.0837	9.4827	0.82097
2.20	+	+	15.9493	15.4885	13.3503	12.3471	12.1170	0.80188
2.20	−	+	16.0665	15.6043	13.4595	12.4498	12.2066	0.80234
2.20	+	−	17.9478	17.4144	14.7624	14.1608	13.6531	0.80267
2.20	−	−	17.8615	17.3222	14.6809	14.0962	13.5831	0.80265

P_T values were 0.728 and 0.710 after 34 hours, respectively. This corresponds to the relaxation times of 1358 hours for P_T^+ and 663 hours for P_T^-. The relative uncertainty of the measured P_T values has been estimated to be ±5 %. This error includes the uniformity meaurements using the NMR data from the three coils.

The configuration of the two neutron intensity monitors M1 and M2 and the three transmission detectors T1, T2 and T3 is shown in Fig. 2. The detectors were of similar design and the electronics were identical [1,2]. Each detector consisted of a CH_2 converter, 60 mm thick, placed behind a large veto scintillation counter A. Charged particles emitted forward were detected by two counters S1 and S2 in coincidence. The monitor converters and S1, S2 counters were 30 mm in diameter and the corresponding elements of the transmission detectors were 90, 92 and 96 mm for T1, T2 and T3, respectively. The NP array, also shown in Fig. 2, was similar as the neutron detectors. The two multiwire proportional chambers behind the converter were protected by its veto A and triggered by S1, S2 and S3 counters in coincidence.

The result of $\Delta\sigma_L$ is independent on the neutron beam intensity, if a probability of quasi-simultaneous detection of two neutrons in one transmission detector may be neglected. The efficiency of detector are then limited and each of the detectors is independent of any other one [1].

Dedicated tests were performed during an additional run with a high intensity unpolarized deuteron beam. Using the same transmission set-up the neutron carbon total cross section $\sigma_{tot}(n-C)$ was determined at $T_{kin}(n) = 1.5$ GeV. For this purpose a number of carbon targets with different thicknesses were inserted in the neutron beam line instead of the PPT. The measured $\sigma_{tot}(n-C)$ value agrees with the data from the compilation "Cross Sections of Particles and Nuclei with Nuclei" [38].

5 Data analysis

For each accelerator cycle the following main information was recorded and displayed by the data acquisition system:

- rates of the two calibrated ionization chambers used as the primary deuteron beam intensity monitors,
- rates of coincidences and accidental coincidences for the two neutron detectors M1 and M2 used as the intensity monitors of the neutron beam incident on the PPT,
- rates of coincidences and accidental coincidences for the three neutron transmission detectors T1, T2 and T3,
- rates of the left and right arms of the *pp* beam polarimeter.

At the beginning of the run, statistics at 2.20 and 1.79 GeV with P_T^- were recorded. Then the data were taken at 2.20, 1.79 GeV and 1.59 GeV with P_T^+. At the latter energy, the data with P_T^- could not be measured.

The recorded data were then analyzed in two steps. In the first step, "bad" files were removed, as well as "empty" cycles and cycles with incorrect labels of P_B signs. The number of "bad" cycles for the cumulated statistics represented a few tenth of percent. Remaining event statistics over the run for different detectors are shown in Table 1, separately for each combination of the $\vec{P}_B$ and $\vec{P}_T$ direction. With decreasing energy σ_{0tot} for all target elements decreases and the global target transmission ratio $\Sigma T/\Sigma M$ increases, as expected. Since the statistics listed in one row were taken simultaneously, we see also a monotonous decrease as a function of the detector distance from the target.

The second step of the data analysis used the previously selected events in order to check the stability of neutron detectors, to determine parameters of the statistical distribution and to obtain the final results. The

Table 2. The measured $-\Delta\sigma_L(np)$ values at different energies for the two opposite target polarizations, for the individual transmission detectors and for the cumulated statistics. The instrumental asymmetry (IA) and the averaged $-\Delta\sigma_L(np)$ data were deduced. The quoted errors are statistical only

T_{kin} (GeV)	Transm. detectors	$-\Delta\sigma_L(P_T^+)$ (mb)	$-\Delta\sigma_L(P_T^-)$ (mb)	IA (mb)	Average $-\Delta\sigma_L$ (mb)
1.59	T1	$+4.7 \pm 3.9$			$+4.7 \pm 3.9$
	T2	$+5.5 \pm 3.9$			$+5.5 \pm 3.9$
	T3	$+2.0 \pm 4.0$			$+2.0 \pm 4.0$
	T1,2,3	$+4.1 \pm 2.9$			$+4.1 \pm 2.9$
1.79	T1	$+0.7 \pm 3.0$	$+2.5 \pm 2.3$	-0.9 ± 1.9	$+1.6 \pm 1.9$
	T2	-4.2 ± 3.1	$+0.2 \pm 2.3$	-2.2 ± 1.9	-2.0 ± 1.9
	T3	-0.9 ± 3.1	-0.3 ± 2.4	-0.3 ± 2.0	-0.6 ± 2.0
	T1,2,3	-1.5 ± 2.2	$+0.9 \pm 1.7$	-1.2 ± 1.4	-0.3 ± 1.4
2.20	T1	$+3.4 \pm 2.1$	$+2.0 \pm 1.8$	$+0.7 \pm 1.4$	$+2.7 \pm 1.4$
	T2	$+4.1 \pm 2.1$	-2.0 ± 1.9	$+3.0 \pm 1.4$	$+1.0 \pm 1.4$
	T3	-0.1 ± 2.1	$+0.4 \pm 1.9$	-0.2 ± 1.4	$+0.1 \pm 1.4$
	T1,2,3	$+2.5 \pm 1.5$	$+0.1 \pm 1.3$	$+1.3 \pm 1.0$	$+1.3 \pm 1.0$

transmission ratios as functions of time were analyzed for each combination of the individual M and T detectors, at any neutron energy and the P_T sign. No significant time dependence of checked values was observed. The results were extracted using the relations (2.5a), (2.5b) and (3.9). Each of them contains a hidden contribution [13] from the instrumental asymmetry (IA) due to the counter misalignments and to the residual perpendicular components in the beam polarization. For this reason a half-sum of (2.7), i.e. a simple average, provides $\Delta\sigma_L$, whereas a half-difference gives the IA value, as has been discussed in [13].

The IA contribution could be hardly suppressed. Due to the longitudinal $\vec{P}_B$ direction and the full kinematic axial symmetry, it is usually small for the $\Delta\sigma_L$ experiment. It may be very large for the $\Delta\sigma_T$ measurement, where no symmetry exists. The results strongly depend on the detector stabilities and their fixed positions over the data acquisition with the both P_T signs. For stable detectors, $\Delta\sigma_L$ is expected to be found time independent and equal for each transmission detector, within statistical errors. In contrast, the IA value depends on each individual neutron detector, including the monitors.

In Table 2 are listed the $-\Delta\sigma_L(np)$ values for both signs of P_T, their half differences and the half-sums. All results were obtained using common statistics from both monitors M1 and M2. The abreviation T1,2,3 signify that the entire statistics from all detectors were taken into account.

It can be seen that IA was considerably smaller for the detectors T1 and T3 than for T2. The IA values change its sign for almost all detectors between 1.79 and 2.20 GeV. Since the elements of the detectors were not moved during the run, we assume that the residual perpendicular components in $\vec{P}_B$ were oposite. The relative normalization and systematic errors, from different sources are summarized as follows:

- Beam polarization including time dependence $\pm$ 1.7 %
- Target polarization ..... $\pm$ 5.0 %
- Number of the polarizable hydrogen atoms including filling mode ..... $\pm$ 1.5 %
- Magnetic field integral of the neutron spin rotator ..... $\pm$ 0.2 %
- Polarization of other atoms ..... $\pm$ 0.3 %
- Inefficiencies of veto counters ..... $\pm$ 0.1 %

- Total of the relative systematic errors ..... $\pm$ 5.5 %
- Absolute error due to the extrapolation of results towards 0° ..... < 0.04 mb

6 Results and discussion

The final $-\Delta\sigma_L(np)$ values are presented in Table 3 and shown in Fig. 3. The statistical and systematic errors are quoted. The total errors are the quadratic sums of both uncertainties. Since the measurement at 1.59 GeV was carried out with one P_T sign only, the instrumental ϕ-asymmetry could not be removed using (7). At this energy, we have added the weighted average of the absolute IA values at 1.79 and 2.20 GeV ($\pm$ 1.18 mb) in quadrature to the systematic error.

The results from [1,2] together with the existing $\Delta\sigma_L(np)$ data [13-18], obtained with free polarized neutrons at lower energies, are also shown in Fig. 3. We added the point at 19.7 MeV recently measured at TUNL [22] in order to show the $\Delta\sigma_L(np)$ energy dependence in a large energy range. The new results smoothly connect with the data at lower and at higher energies and suggest even faster decrease above 1.1 GeV than previously

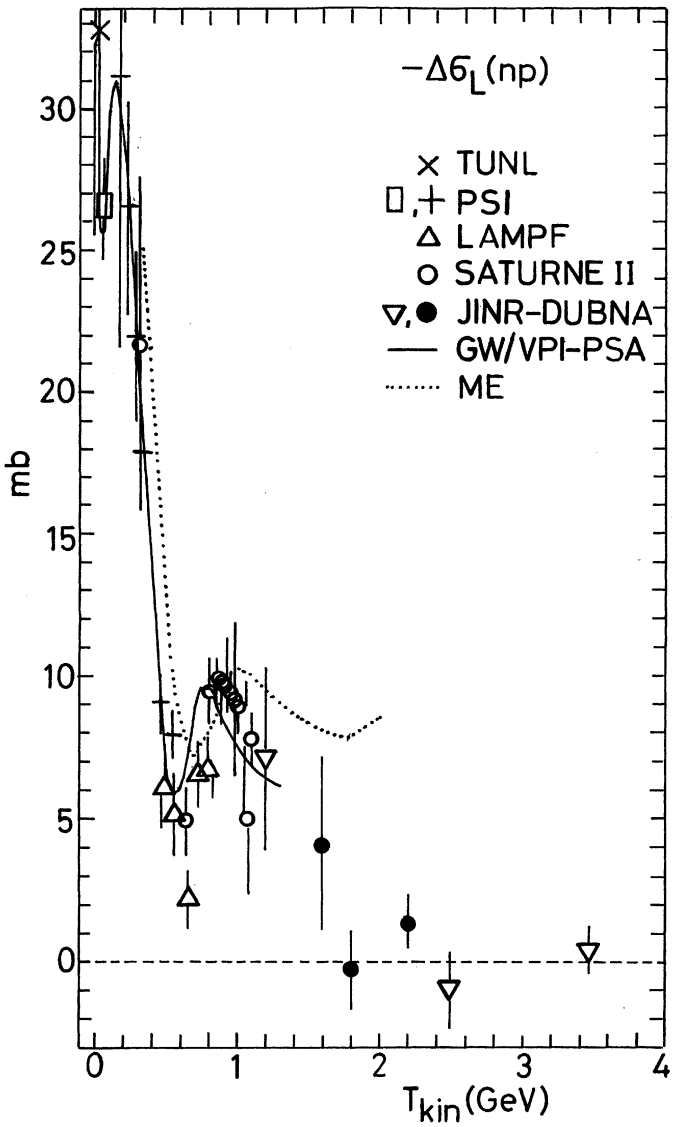

Fig. 3. Energy dependence of $-\Delta\sigma_L(np)$. The meaning of the symbols: • ... this experiment, ▽ ... JINR [1,2], × ... TUNL [22], rectangle ... PSI [18], + ... PSI [16], △ ... LAMPF [17], ○ ... SATURNE II [13,14], full curve ... GW/VPI-PSA [24] (SP99 solution), dotted curve ... meson-exchange model [41]

observed [1,2]. The solid curve represent the energy dependent GW/VPI-PSA [24] (SP99 solution) fit of this observable over the interval from 0.02 to 1.3 GeV. Above 0.8 GeV the fit considerably differs from that presented in [1,2]. This is due to a large amount of *np* and *pp* data points for different observables, included into the GW/VPI-PSA database. The database also contains the previous JINR $\Delta\sigma_L(np)$ result at 1.19 GeV. Unfortunately, the number of $\Delta\sigma_L(np)$ points is too small with respect to a prevalence of all other scattering data. Consequently the energy dependent GW/VPI-PSA fit is only in a qualitative agreement with the measured values. Above 1.1 GeV (SATURNE II) the *np* database is insufficient at all. Nevertheless, the high energy part of the PSA fit follows fairly well the behaviour of the experimental data.

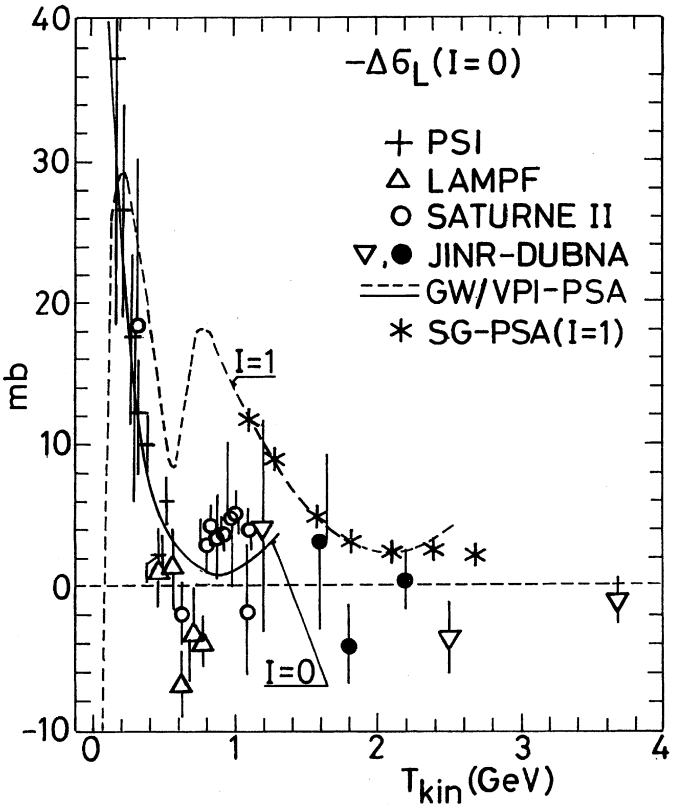

Fig. 4. Energy dependence of the $-\Delta\sigma_L(I=0)$ calculated from measured *np* data and the known *pp* values. The *np* data at the same energies as in Fig. 3 are used and the $I=0$ results are denoted by the same symbols. The full line is calculated from the common *np* and *pp* GW/VPI-PSA [24] (SP99 solution). The dashed line is the $-\Delta\sigma_L(I=1)$ prediction from the same GW/VPI-PSA, and ($\star$) are $I=1$ predictions from SG-PSA [29]

Using (2.11), one can deduce $\Delta\sigma_L(I=0)$ values from the obtained $\Delta\sigma_L(np)$ results and the existing $\Delta\sigma_L(pp)$ data. For this purpose, we used the ANL-ZGS [39] and SATURNE II [40] $\Delta\sigma_L(pp)$ data. The results are given in Table 4 and plotted in Fig. 4. Since the *pp* data are accurate, the $-\Delta\sigma_L(I=0)$ values have roughly two times larger errors than the *np* results. For this reason, an improved accuracy of *np* measurements is important.

In Fig. 4 are also plotted the $-\Delta\sigma_L(I=0)$ values from [1,2] together with those using the $\Delta\sigma_L(np)$ data sets [13-17]. All results are compatible and suggest a plateau or a maximum around 1.5 GeV, followed by a rapid decrease with increasing energy. The solid curve was calculated from the *np* and *pp* GW/VPI-PSA fits. An apparent disagreement with the measured data points above 0.6 GeV is related to a fairly rough PSA description of *np* data. The difference between the GW/VPI-PSA fit and the data, shown in Fig. 3, increases twice for the $I=0$ energy dependence in Fig. 4.

In the same figure are plotted the $-\Delta\sigma_L(I=1)$ PSA fits for a comparison. The GW/VPI-PSA for *pp* elastic scattering cover the energy range up to 2.55 GeV (dashed line) and SG-PSA up to 2.7 GeV (stars above 1.1 GeV).

Table 3. The final $-\Delta\sigma_L(np)$ results. Total errors are quadratic sums of the statistical and systematic ones. The energy and the laboratory momenta of the neutron beam in the production target center are given

T_{kin} (GeV)	p_{lab} (GeV/c)	$-\Delta\sigma_L(np)$ (mb)	Statis. error (mb)	System. error (mb)	Total error (mb)
1.59	2.35	+4.1	±2.9	±1.20	±3.1
1.79	2.56	−0.3	±1.4	±0.02	±1.4
2.20	2.99	+1.3	±1.0	±0.07	±1.0

Table 4. The $-\Delta\sigma_L(I=0)$ values deduced from the present $\Delta\sigma_L(np)$ results and existing $\Delta\sigma_L(pp)$ data. The energies of $\Delta\sigma_L(pp)$ data and corresponding references are also listed

$T_{kin}(np)$ (GeV)	$T_{kin}(pp)$ (GeV)	$-\Delta\sigma_L(pp)$ (mb)	Ref. pp	$-\Delta\sigma_L(I=0)$ (mb)
1.59	1.594	$+4.93 \pm 0.30$	[40]	$+3.2 \pm 6.2$
1.79	1.798	$+3.39 \pm 0.10$	[40]	-4.0 ± 2.8
2.20	2.176	$+2.28 \pm 0.10$	[39]	$+0.3 \pm 2.0$

Both PSA contain almost all existing data and their predictions at low energies are in excellent agreement.

Some dynamic models predicted the $\Delta\sigma_{L,T}$ behaviour for np and pp transmissions. Below 2.0 GeV, an usual meson exchange theory of NN scattering [41] gives the $\Delta\sigma_L(np)$ energy dependence as shown by the dotted curve in Fig. 3. It can be seen that this model provides only a qualitative description at low energies and disagree considerably with the data above 1 GeV.

In [1,2] was discussed a model of a nonperturbative flavour-dependent interaction between quarks, induced by a strong fluctuation of vacuum gluon fields, i.e. instantons. An energy dependent contribution to $\Delta\sigma_L(np)$ was qualitatively estimated. Concerning this model we refer to [1,2] and to references therein, since no new relevant predictions are available.

The investigated energy region corresponds to a possible generation of heavy dibaryons with masses $M > 2.4$ GeV (see review [42]). For example, a model [43,44] predicts the formation of a heavy dibaryon state with a color octet-octet structure.

The possible manifestation of exotic dibaryons in the energy dependence of different pp and np observables was predicted by another model [45-49]. The authors used the Cloudy Bag Model and an R-matrix connection to long-range meson-exchange force region with the short-range region of asymptotically free quarks. The model gives the lowest lying exotic six-quark configurations in the isosinglet and the spin-triplet state $^3S_1$ with the mass M = 2.63 GeV ($T_{kin} = 1.81$ GeV). For the $I = 0$ state, the $^3S_1$ partial wave is expected to be predominant. The measurement of $\Delta\sigma_T$ observable for np transmission and its determination for $I = 0$ may provide a significant check. Since $\Delta\sigma_T$ for arbitrary isospin state contains no uncoupled spin-triplet state, a possible dibaryon resonance effect in $^3S_1$ may be less diluted. Moreover, in the difference of both quantities the spin-singlet contributions vanish.

The three optical theorems determine the imaginary parts of the nonvanishing forward amplitudes as shown in (2.8) to (2.10). A maximum in $I = 0$ amplitudes or in their combinations dominated by the spin-triplet states will be a necessary condition for the predicted resonance. The sufficient condition may be provided by real parts. For np scattering they can be determined by measurements of observables in the experimentally accessible backward direction, as was shown in [50].

The $I = 0$ spin dependent total cross sections represent a considerable advantage for studies of possible resonances. This is in contrast with the $I = 1$ system where the lowest lying exotic six-quark configuration corresponds to the spin-singlet state $^1S_0$. This state is not dominant and is hard to be separated it in the forward direction. Scattering data directly related with the spin-singlet amplitude at other angles are preferable to be measured.

7 Conclusions

The new results are presented for the transmission measurements of the $\Delta\sigma_L(np)$ energy dependence in the Dubna Synchrophasotron energy region below 3.7 GeV. Measured $\Delta\sigma_L(np)$ values are compatible with the existing np results, using free neutrons. The rapid decrease of $-\Delta\sigma_L(np)$ values from 1.1 to 2.0 GeV is confirmed. It is found to be faster than expected from the previous measurement.

The $\Delta\sigma_L(I = 0)$ quantities, deduced from the measured $\Delta\sigma_L(np)$ values and the existing $\Delta\sigma_L(pp)$ data, are also presented. They indicate a plateau or a maximum around 1.5 GeV, followed by a rapid decrease with energy.

Obtained results are compared with the dynamic model predictions and with the recent GW/VPI-PSA fit. A necessity of further $\Delta\sigma_L(np)$ measurements and new $\Delta\sigma_T(np)$ data in the kinetic energy region above 1.1 GeV is emphasized.

Acknowledgements. Authors thank the JINR LHE and LNP directorates for support of these investigations. Discussions with V.N.Penev and B.Peyaud solved several problems. We are grateful to J.Ball, M.P.Rekalo and I.I.Strakovsky for helpful suggestions.

The measurements were possible due to the JINR directorate Grant. The work was supported in part by the International Science Foundation and Russian Government through Grant No. JHW 100, by the International Association for the Promotion of Cooperation with Scientists from the Independent States of the Former Soviet Union (INTAS) through Grant No. 93-3315, by the Russian Foundation for Basic Research through Grants RFBR-93-02-03961, RFBR-93-02-16715, RFBR-95-02-05807, RFBR-96-02-18736 and by the Fundamental Nuclear Physics Foundation Grant 122.03.

References

1. B.P. Adiasevich, et al., Zeitschrift für Physik C **71**, 65 (1996)
2. V.I. Sharov, et al., JINR Rapid Communications **3[77]-96**, 13 (1996)
3. F. Lehar, et al., Nucl.Instrum.Methods A **356**, 58 (1995)
4. N.A. Bazhanov, et al., Nucl.Instrum.Methods A A **372**, 349 (1996)
5. I.B. Issinsky, et al., Acta Physica Polonica B **25**, 673 (1994)
6. A. Kirillov, et al., "Relativistic Polarized Neutrons at the Laboratory of High Energy Physics, JINR", Preprint JINR E13-96-210, Dubna, 1996
7. E.V.Chernykh, S.A.Zaporozhets, Proceedings of the ES-ONE International Conference "RTD 94", Editors R.Pose, P.U. ten Kate, E.W.A.Lingeman, Preprint E10,11-95387, JINR, Dubna 1995, p.179
8. N.G. Anischenko, et al., JINR Rapid Communications **N6[92]-98**, 49 (1998)
9. D.P. Grosnick, et al., Phys.Rev. D **55**, 1159 (1997)
10. C.Lechanoine-Leluc, F.Lehar, Rev.Mod.Phys. **65**, 47 (1993)
11. I.P.Auer, et al., Phys.Rev.Lett. **46**, 1177 (1981)
12. W.Grein, P. Kroll, Nucl. Phys. A **377**, 505 (1982)
13. F.Lehar, et al., Phys.Lett. **189B**, 241 (1987)
14. J.-M. Fontaine, et al., Nucl.Phys. B **358**, 297 (1991)
15. J.Ball, et al., Zeitschrift für Physik C **61**, 53 (1994)
16. R.Binz, et al., Nucl.Phys. A **533**, 601 (1991)
17. M. Beddo, et al., Phys.Lett. **258B**, 24 (1991)
18. P.Haffter, et al., Nucl.Phys. A **548**, 29 (1992)
19. J. Brož, et al., Zeitschrift für Physik A **359**, 23 (1997)
20. W.S.Wilburn, et al., Phys.Rev. C **52**, 2352 (1995)
21. J.Brož, et al., Zeitschrift für Physik A **354**, 401 (1996)
22. J.R.Walston, PhD Thesis, North Carolina State University, 1998 (unpublished)
23. B.W.Raichle, PhD Thesis, North Carolina State University, 1997 (unpublished)
24. R.A.Arndt, et al., Phys.Rev. C **56**, 3005 (1997)
25. J.Bystrický, F.Lehar, P.Winternitz, J.Physique (Paris) **39**, 1 (1978)
26. S.M.Bilenky, R.M.Ryndin, Phys.Lett. **6**, 217 (1963)
27. R.J.N.Phillips, Nucl.Phys. **43**, 413 (1963)
28. J. Ball, et al., Nuovo Cimento A **111**, 13 (1998)
29. J.Bystrický, C.Lechanoine-LeLuc, F.Lehar, Eur.Phys.J. C **4**, 607 (1998)
30. V.G. Ableev, et al., Nucl.Instrum.Methods A **306**, 73 (1991)
31. L.S.Azhgirey, et al., Pribory i Tekhnika Experimenta **1**, 51 (1997), transl. Instrum. and Exp.Techniques **40**, 43 (1997)
32. N.A. Bazhanov, et al., Nucl.Instrum.Methods A **402**, 484 (1998)
33. V.G.Ableev, et al., Nucl. Phys. A **393**, 941 (1983) and A **411** 541E (1983)
34. E.Cheung, et al., Phys.Lett. B **284**, 210 (1992)
35. A.A. Nomofilov, et al., Phys.Lett. B **325**, 327 (1994)
36. V.Ghazikhanian, et al., Phys.Rev. C **43**, 1532 (1991)
37. E.I.Bunyatova, R.M.Galimov, S.A.Luchkina, "Investigation of Stable Paramagnetic HMBA Complex in Different Solvents", Preprint JINR 12-82-732, Dubna 1982
38. V.S.Barashenkov, "Secheniya Vzaimodeistviya Chastits i Yader s Yadrami." JINR Publishing Department, Dubna, 1993
39. I.P.Auer, et al., Phys.Rev.Lett. **41**, 354 (1978)
40. J.Bystrický, et al., Phys.Lett. **142B**, 141 (1984)
41. T.-S.H.Lee, Phys.Rev. C **29**, 195 (1984)
42. I.I.Strakovsky, Fiz. Elem. Chastits At. Yadra **22**, 615 (1991), transl. Sov.J.Part.Nucl. **22**, 296 (1991)
43. B.Z.Kopeliovich, F.Niedermayer, Zh.Eksp.Teor.Fiz. **87**, 1121 (1984), transl. Sov.Phys. JETP **60**(4), 640 (1984)
44. B.Z.Kopeliovich, Fiz. Elem. Chastits At. Yadra **21**, 117 (1990), transl. Sov.J.Part.Nucl. **21**(1), 49 (1990)
45. P.LaFrance, E.L.Lomon, Phys.Rev. D **34**, 1341 (1986)
46. P.Gonzales, P.LaFrance, E.L.Lomon, Phys.Rev. D **35**, 2142 (1987)
47. P.LaFrance, Can.J.Phys. **68**, 1194 (1990)
48. E.L. Lomon, Colloque de Physique (France) **51**, C6-363 (1990)
49. P. LaFrance, E.L. Lomon, Proceedings of the International Conference "Mesons and Nuclei at Intermediate Energies", Dubna, 3-7 May 1994, Editors: M.Kh. Khankhasaev, Zh.B. Kurmanov, World Scientific, Singapore, 1995-XV, p.97
50. J. Ball, et al., Eur.Phys.J. C **5**, 57 (1998)